5-2024

Development and Evaluation of an Arsenic Transport Model for the Maurice River Watershed

Christina Eddleman
eddlema@clemson.edu

DEVELOPMENT AND EVALUATION OF AN ARSENIC TRANSPORT MODEL FOR THE MAURICE RIVER WATERSHED

A Thesis
Presented to the Graduate School of
Clemson University

In Partial Fulfillment
of the Requirements for the Degree
Master of Science Civil Engineering

---

by
Christina X. Eddleman
May 2024

Accepted by:
Dr. Abdul Khan, Committee Chair
Dr. Earl Hayter
Dr. Brian Powell

ABSTRACT

For many Superfund sites across the United States, arsenic is one of the most common contaminants of concern that must be cleaned up to protect human and environmental health. Past research and health studies have documented the harmful effects of inorganic arsenic on humans and the environment but selecting an appropriate remediation plan depends on several site-specific factors at each Superfund site. To assist in determining an appropriate remediation plan, sediment and contaminant transport models have been used to simulate the transport of arsenic and other contaminants of concern at contaminated sites to, e.g., make relative comparisons of the efficacy of different proposed remedial alternatives. This thesis describes a) the development of a three-tier contaminant fate and transport modeling system and b) the application of the model to a portion of the Maurice River watershed which includes the Vineland Chemical Superfund site in Vineland, NJ. This site is adjacent to the Blackwater Branch, a tributary of the Maurice River. This thesis also demonstrates the application of a speciation model, PHREEQC, which calculates the inorganic species of arsenic, arsenate and arenite using site-specific data from an arsenic contaminated unconfined aquifer on the Vineland Chemical site. This model serves as an important tool to assess the arsenic toxicity present at this site.

After developing and partially calibrating the three-tier modeling system, the model was used to demonstrate its ability to simulate two potential remediation alternatives for the Vineland Chemical Superfund site. The first alternative did not include any remediation except for the sediments and floodplain soils previously removed from Blackwater Branch. The second alternative included the remediated Blackwater Branch and dredging the contaminated sediments in the Maurice River from the confluence with this tributary down to Almond Road. In both alternatives, the arsenic concentration in the water column decreased throughout the model domain as the flow transported the contaminant further downstream. As for the arsenic concentration in the sediment bed approximately 1 mile [1.6 km] downstream of the confluence of the Blackwater Branch and Maurice River, both alternatives showed

the exact same results concluding that the short simulation period used for this demonstration was not sufficient for comparing the long-term effectiveness of each alternative. In both alternatives, the arsenic concentration in the top layer of the sediment bed decreased as arsenic diffused into the water column and less contaminated sediment from upstream deposited onto the bed. Despite the limited data available to calibrate the three-tier modeling system and the shortness of the six-month simulations, the model results showed that quantitatively the model behaved as expected. Across the model domain, the average arsenic concentration in the sediment bed only reduced by one percent indicating that there was no significant concentration of arsenic transported downstream into Union Lake. The small percent of arsenic that was suspended and transported downstream was transported during high flow events in its colloidal bound phase and freely dissolved phase indicating that most of the arsenic sorbed to solids remained in the sediment bed. The results from PHREEQC indicated that the 16 groundwater samples collected from the Vineland Chemical Superfund site dominantly consisted of arsenate, the less toxic form of arsenic. The arsenic sorbed to the iron minerals present in the aquifer rather than dissolving into the groundwater. These results showed that there was less risk to humans because the arsenic was sorbed to the iron minerals in the aquifer and therefore less mobile.

This research demonstrated that the three-tier modeling system and PHREEQC are useful tools with separate applications, but with further investigation, future studies may use PHREEQC and contaminant transport model like that used in this study in conjunction to predict which species of arsenic are present in a highly contaminated area (hotspot) of the model domain. This could improve current arsenic transport modeling capabilities because existing arsenic transport models cannot simulate or identify arsenic species to better characterize the level of arsenic toxicity.

ACKNOWLEDGEMENTS

I would like to thank Dr. Khan, Dr. Powell, and Dr. Hayter for providing challenging, insightful coursework that allowed me to further develop my skillset as a civil/environmental engineer. I would like to thank the United States Army, Engineer Research and Development Center for providing me with the opportunity to pursue and complete this research. I would like to thank Dr. Powell for introducing me to speciation modeling, as well as guiding me through my research related to arsenic speciation. I would like to thank Dr. Khan for providing challenging coursework that tested and improved my understanding of fundamental concepts related to fluid mechanics and open channel flow. I would like to thank Dr. Hayter for providing the opportunity to conduct research on the contaminant transport modeling with the inclusion of contaminant speciation. Not only has he been a great mentor throughout my time at Clemson, but he has also shared his wealth of knowledge, his abundant support and patience, and his commitment to developing the next generation of sediment transport modelers. I am grateful for working and learning from Dr. Hayter and hope that I can continue his legacy in the world of sediment transport modeling.

TABLE OF CONTENTS

LIST OF TABLES & FIGURES

I. INTRODUCTION

The United States Environmental Protection Agency (USEPA) is responsible for managing the cleanup of hundreds of Superfund sites. One of the most prominent contaminants at these sites is arsenic. This contaminant is commonly found is soil and water (drinking water sources) and is known to cause skin lesions, rashes, and cancer over long-term exposure (WHO, 2024). The development of a long-term remediation plan to remove arsenic is dependent on several factors and may take years to develop. Numerical models are one of the tools commonly used to help decide what remedial action should be undertaken. Numerical models are powerful tools capable of simulating hydrodynamics, sediment transport, and contaminant transport within a waterbody. They have been commonly used to evaluate and compare potential remediation plans to determine which proposed plan is most effective. As discussed later in this chapter, a three-tier contaminant fate and transport modeling system for the area surrounding the Vineland Chemical Company Superfund site in Vineland, NJ (Figure 1) was developed and applied in this thesis. The modeling system includes a watershed loading modeling, a groundwater discharge model, and an in-stream hydrodynamic, sediment transport, and contaminant fate and transport model. Once calibrated, the three-tier model was used to simulate two potential remediation plans for six months to compare the simulated total arsenic transported throughout the EFDC+ model domain.

Additionally, the USEPA conducts risk assessments at contaminated sites like Vineland Chemical to characterize the nature and magnitude of risks to human and the environment. As discussed later in this chapter, a geochemical model, pH-Redox-Equilibrium (PHREEQC), was used with site-specific data to demonstrate how this tool can improve our understanding of the arsenic toxicity associated with the Vineland Chemical Superfund site. While no modeling tool is perfect, the three-tier modeling system and PHREEQC are useful tools for decision makers, engineers, and scientists that work to develop effective long-term remediation plans.

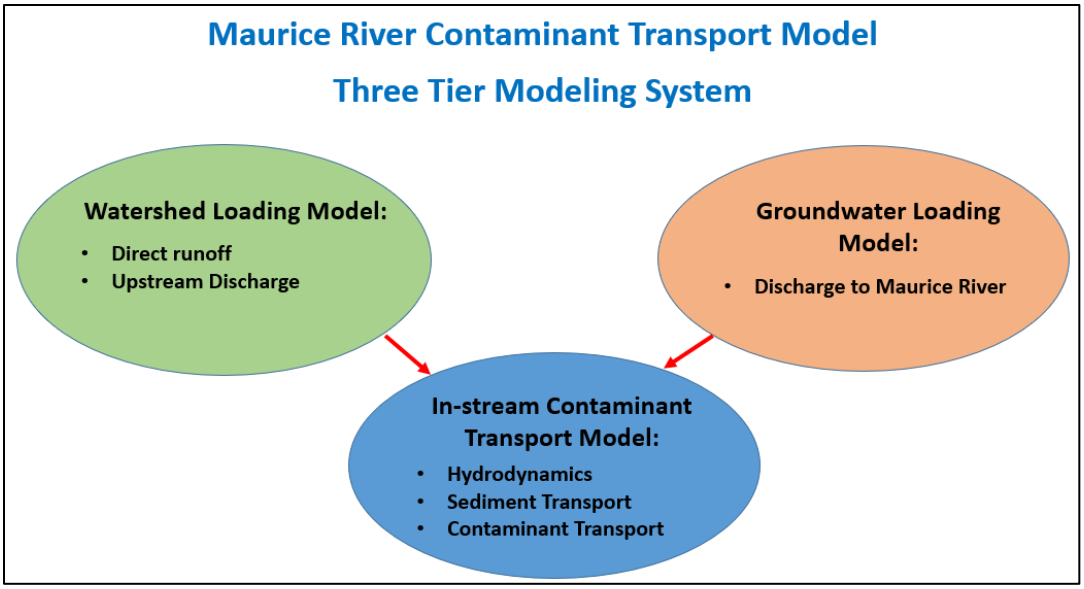

Figure 1: Three-Tier Modeling Study Flow Diagram

PROBLEM STATEMENT

The potential mobilization of arsenic is dependent on the composition of the soil, sediments, surface water, and groundwater quality. Thus, understanding the behavior of arsenic is important to develop an effective long-term remediation plan at each arsenic-contaminated Superfund site. Common treatment techniques include pump and treat, in-situ remediation (e.g., air sparge), ion exchange, among others; however, these treatment techniques can be expensive so conducting a Remediation Investigation (RI) and developing numerical models can be useful for decision makers to select the most effective remediation plan for each site.

Additionally, arsenic-contaminated Superfund sites should consider investigating which species of arsenic are present onsite to better understand the level of toxicity and potential risk to human health and the environment. Typically, there are two forms of inorganic arsenic present: arsenite (As(3)) and arsenate (As(5)). Both forms of arsenic have been identified at Vineland Chemical Company and have different toxicity risks and mobilization behaviors that can impact the distribution of the arsenic contamination. As(3), is the reduced form of arsenic that is more soluble and commonly found in groundwater. This creates a higher risk to human health because much of society depends on groundwater as a drinking water source. As(5), is the oxidized form of arsenic that is more commonly found sorbed to sediments and considered the more stabilized, less toxic form of arsenic.

GOAL AND OBJECTIVES

The first goal is to develop and evaluate a three-tier contaminant fate and transport modeling system to simulate the transport of total arsenic in the Maurice River. To achieve this goal, the following objectives will be completed:

Develop a three-tier contaminant fate and transport modeling system which includes the dynamically linked Environmental Fluid Dynamics Code (EFDC+) hydrodynamic, sediment transport, and contaminant transport surface water modeling system developed by Dynamic Solutions International (DSI), LLC (DSI LLC, 2020); the watershed loading model, Hydrologic Simulation Program Fortran (HSPF) (Donigian Jr., Bicknell, & Imhoff, 1995); and the groundwater model, Clemson University Hydrograph (CU Hydrograph) (Murdoch, 2023). Then calibrate the three-tier contaminant fate and transport model using existing measured data, and then use it to simulate two potential remediation alternatives and compare results.

The second goal is to demonstrate PHREEQC's ability to calculate arsenic speciation with site-specific data and discuss implications for future contaminant transport modeling studies. The purpose of using PHREEQC is to determine what species of arsenic are present at the selected groundwater monitoring wells to characterize the level of toxicity and risk to human health and the environment. To achieve this goal, the following objective will be completed:

Demonstrate how PHREEQC is used to calculate the fraction of As(3) and As(5) present in 16 groundwater monitoring wells at the Vineland Chemical Superfund site. These results can be used to better understand the potential human health risks and what remediation strategies are best suited to clean up the site.

The next two sections have background information on the Superfund Sites in the Maurice River watershed and the Maurice River system itself.

VINELAND CHEMICAL AND FORMER KIL-TONE SUPERFUND SITES

The Vineland Chemical Company Superfund site is located in Vineland (Cumberland County), New Jersey. The Vineland Chemical Company operated in the 1900s and produced arsenical herbicides and fungicides until 1994. The company mishandled the byproduct arsenic salts, and as a result, arsenic contaminated soils, sediment, surface water, and groundwater have been found. The Vineland Chemical Company was added to the National Priorities List (NPL) on September 1, 1984. The site is divided into six operable units (OU) with specific remedy action plans assigned to each OU as shown in Figure 2. OU1 included the source material control at the Superfund site. Arsenic-contaminated soil was cleaned using a soil washing facility. According to (USEPA, 2024), the facility "processed 70 tons of excavated soil per hour. The facility processed over 400,000 tons of arsenic-contaminated soil and sediment, and the remaining waste was disposed of at a permitted off-site disposal facility. The soil remedy was completed in 2014". OU2 included the management of the migration of arsenic through groundwater. EPA constructed a system to pump out and treat about two million gallons of contaminated groundwater daily. The system began operating in 2000 and continues today on a smaller scale (USEPA, 2024). OU3 addressed contamination of the sediment/soil in the Maurice River, the BWB, and their associated floodplains. Removal of contaminated floodplain soil and sediment was completed in 2012. However, portions of the BWB floodplain have been re-contaminated with arsenic "above the cleanup goals identified in the 1989 ROD due to arsenic in groundwater reaching the sediment/soil during the ongoing implementation of the OU2 remedy" (USEPA, 2024). A remediation system evaluation (RSE) report (GeoTrans, Inc., 2011) found success with the pump and treat (P&T) remedy in protecting BWB. However, the RSE also found that "the pump and treat system was unlikely to restore the aquifer within a reasonable time period as specified by the record of decision". The RSE provided recommendations to optimize/replace the system, and in 2015, an air sparge pilot study was selected to immobilize arsenic in-situ after a series of bench scale treatability studies were conducted (Sehayek et al., 2014).

OU4 includes Union Lake, an 870-acre impoundment on the Maurice River. Arsenic has been found in the sediment bed of this recreational lake. According to (USEPA, 2024), “The upstream remedial activities will be evaluated prior to proceeding with active cleanup of the lake. To date, no unacceptable risks to beach users have been identified”. OU5 included the demolition of eight buildings on site in 1984. OU6 covers the management of saturated soils near the plant site along the BWB tributary. Data collected during the Remedial Investigations of OU2, OU3, OU4, and OU6 support this research.

The former Kil-Tone Company Superfund site is located in Vineland, NJ, approximately 2.5 miles [4 km] southeast of Vineland Chemical Company Superfund site along the Tarkiln Branch tributary, which is a tributary of the Parvin Branch (Figure 3). The former Kil-Tone Company manufactured arsenic-based pesticides from the late 1910s to the late 1930s (USEPA, 2024b). The contaminants of concern include arsenic, copper, and lead, all of which have been identified in the soil, sediments, surface water, and groundwater surrounding the site. The Former Kil-Tone Company was added to the NPL on April 5, 2016 (USEPA, 2024b). The site is divided into four OUs, and data collected in OU4 (Tarkiln Branch and associated floodplains) support this research effort. The Former Kil-Tone Company Superfund site is included in the model domain; however, for this research, the arsenic from the Vineland Chemical Superfund site is the only contaminant addressed in the model.

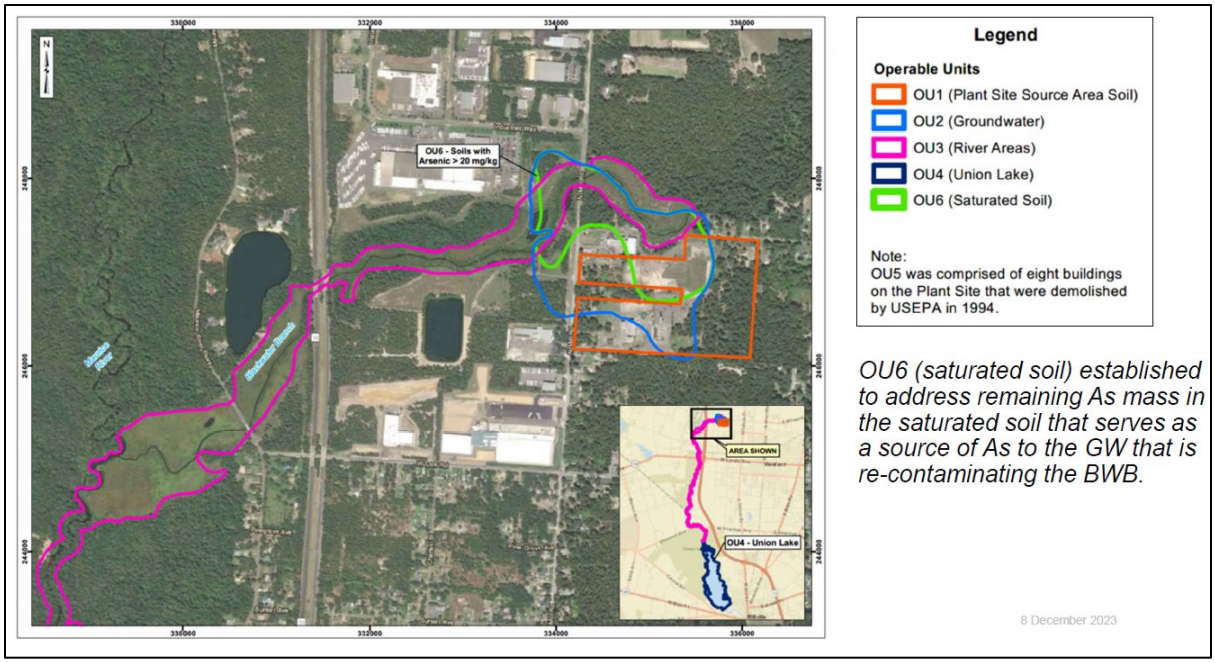

Figure 2: Operable Units of Vineland Chemical Company Superfund Site (ARCADIS, 2023)

MAURICE RIVER AND TRIBUTARIES

The Maurice River watershed is located in the southern coastal plains of New Jersey. The Maurice River watershed drains approximately 384 square miles [994.6 square km]of the eastern portions of Salem and Gloucester Counties, and all of Cumberland County. The watershed is tied to the Cohansey-Kirkwood Aquifer system, an important recharge area and a primary groundwater resource for the region which is used for drinking water either through private or municipal wells. The Maurice River and tributaries included in this study are highlighted in Figure 3c. The Maurice River is the primary hydraulic conduit in the watershed. There are two hydraulic structures along the Maurice River included in the EFDC+ model domain. The Union Lake Spillway and Almond Road Weir are shown in Figure 3a and Figure 3b, respectively. The river extends 30 miles [48.28 km] down gradient from the headwaters in Salem and Gloucester Counties, through Cumberland County, and eventually discharges into Delaware Bay. The river flows in a southerly direction with an average flow of 183.6 cubic feet per second (cfs) [5.2 cubic meters per second (cms)] (USGS, 2024) and receives water from runoff during rainfall events, groundwater discharge, and the surrounding tributaries before flowing over the Union Lake Spillway. The EFDC+ model domain represents the physical area shown in Figure 4a. The upstream boundaries of the model domain include the Maurice River at Garden Road, the BWB at Delsea Road, and the headwaters of the Tarkiln and Parvin Branches. The downstream boundary of the model domain is the Union Lake Spillway. Figure 4a highlights Almond Road because this is the location of the single USGS gage in the model domain. This gage provided continuous measured discharge data from 2012-2015 which were used for the calibration of the HSPF and hydrodynamic models. Figures 4b – 4d provide zoomed in views of the upstream, Almond Road, and downstream boundary to see the individual curvilinear grids that make up the model domain.

The BWB is a 2.5-mile [4 km] Maurice River tributary that runs through the Vineland Chemical Company Superfund site. The BWB cleanup (2006-2012) was part of OU3 and included arsenic removal

from BWB surface water, exposed sediment/soil, and submerged sediments. The Parvin Branch is a small tributary that flows directly into the Maurice River. The Parvin Branch is segmented into the Lower Parvin (1-mile long [1.6 km]) and Upper Parvin (3.2-miles long [5.15 km]). The Lower Parvin begins at the confluence with the Tarkiln Branch and ends at the confluence with the Maurice River. The Upper Parvin begins in a residential area of Vineland and ends at the confluence with the Tarkiln Branch. The former Kil-Tone Company Superfund site is located along the Tarkiln Branch (2-miles long [3.2 km]). Both tributaries are shallow, and the Tarkiln Branch acts as a drainage channel with intermittent flows during rain events.

Figure 3: 3a – Union Lake Spillway, 3b – Almond Road Weir, 3c - Maurice River and Tributaries

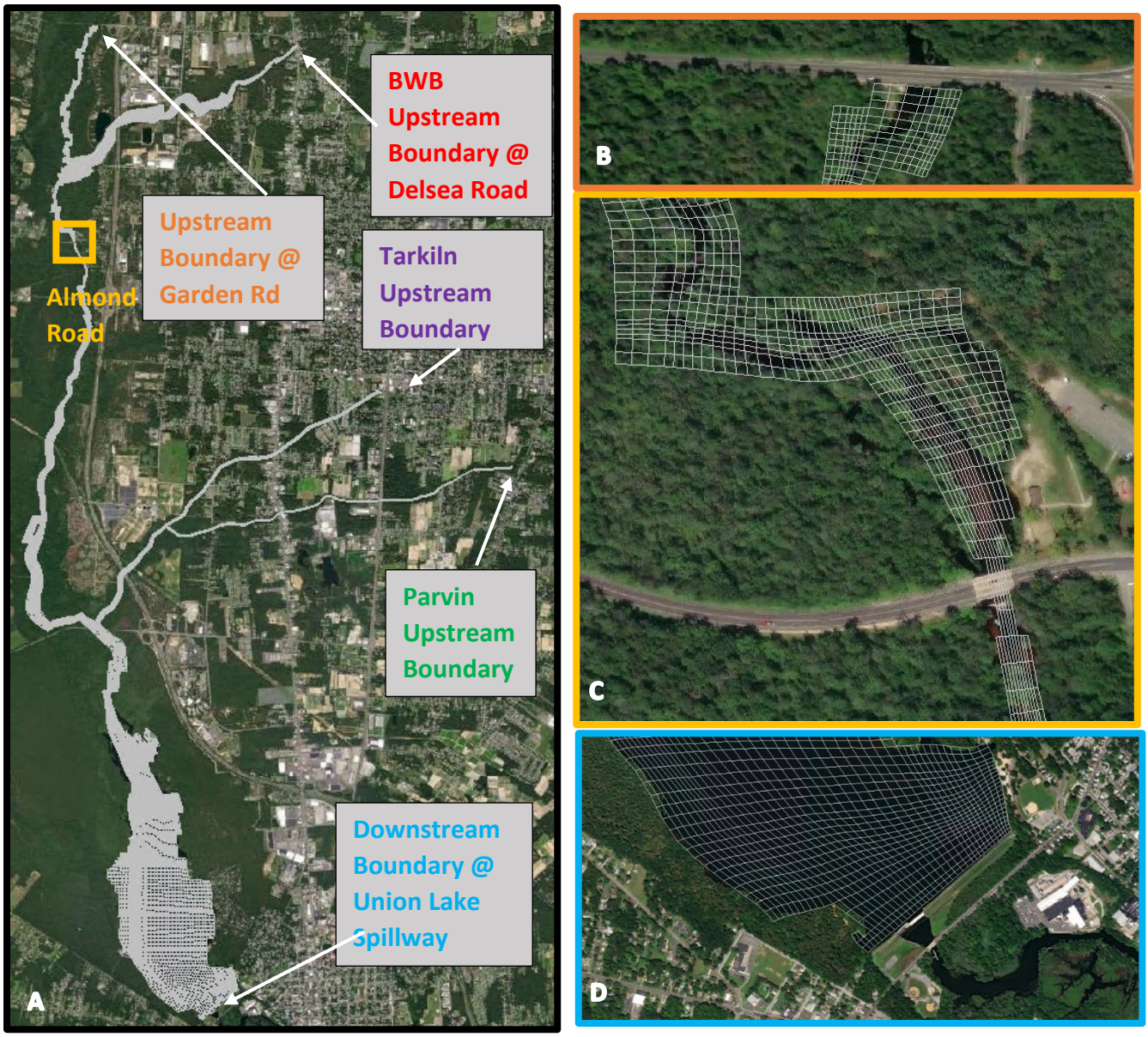

Figure 4: 4a - EFDC+ Model Domain, 4b – Upstream Boundary at Garden Road with Grid Cells in White, 4c – Almond Road with Grid Cells in White, 4d – Downstream Boundary at Union Lake Spillway with Grid Cells In White

II. LITERATURE REVIEW

This literature review focuses on the application of contaminant transport models at similar contaminated sites, and prior investigations performed at the Vineland Chemical Superfund site. This review of models and prior studies at Vineland is performed to enhance the reader's understanding of the current research and its potential to improve existing contaminant transport models.

CONTAMINANT TRANSPORT MODELS

This first section describes contaminant transport models and speciation models applied to contaminated sites similar to the Vineland Chemical Superfund site.

Hayter et al. (2006) published a report evaluating the contaminant transport model, Environmental Fluid Dynamics Code (EFDC), which is an older version of EFDC+. The EFDC model is a public domain, surface water modeling system incorporating fully integrated hydrodynamics (Hamrick, 1992). The EFDC model described in this paper was set up for the Housatonic River, MA where an 11-year simulation of sediment and PCB transport and fate was completed. After running the hydrodynamic model and setting up the sediment transport model, the contaminant transport model component of EFDC was set up using site-specific data, e.g., PCB partition coefficients in the pore water and water column (WC). EFDC's contaminant transport model partitions contaminants into three phases: freely dissolved, particulate, and colloidal bound. An analysis of water column partitioning data indicated that a three-phase partitioning model, like EFDC, is a reasonable representation for partitioning in the water column (WESTON, 2004). The total suspended solids (TSS) and total PCB concentrations from the model were compared to performance measures determined in the modeling study's quality assurance project plan (QAPP). The EFDC model was within the performance measure for both TSS (-27.12%) and PCB concentration (-3.32). The evaluation of the modeling results showed that EFDC can simulate the transport and resultant concentrations of total suspended solids (TSS) and PCBs in the Housatonic River.

Limited PCB and TSS data were collected for this effort, so minimal calibration was completed. Despite the limited data, the results indicated there was reasonable agreement between the simulated and measured PCB and TSS concentrations. A statistical summary of the performance of the EFDC model for TSS and total PCB concentrations was completed based on the modeling study's Quality Assurance Project Plan (QAPP) which created model performance measures for TSS and total PCB. The EFDC model results fell within the established model performance measure for TSS and total PCB (+/- 30%). The purpose of this modeling effort was to evaluate the ability of EFDC to simulate the transport and fate of a contaminant for at least 10 years. The paper concluded "EFDC model's performance, as quantified by the relative bias and the median relative error, is considered good. This demonstrates that EFDC is a robust modeling system that can be successfully implemented at other contaminated sediment sites" (Hayter et al. 2006). EFDC+, a newer version of EFDC, was selected to simulate the fate and transport of arsenic at the Vineland Chemical Superfund site because of the extensive evaluation completed on EFDC, its robustness, and capability to simulate dynamically linked hydrodynamic, sediment transport, and contaminant transport.

A similar modeling study using EFDC was performed for the New Bedford Harbor Superfund Site in Massachusetts by Hayter et al. (2014). New Bedford Harbor is a vertically well-mixed estuary. This modeling study involved creating a "new PCB transport and fate model that will allow multi-decade evaluation of post-remediation conditions in New Bedford Harbor for three different remediation scenarios" (Hayter et al. 2014). The procedure to set up, calibrate, and run EFDC is the same as that used the current research for EFDC+. First the hydrodynamic model was set up and calibrated using measured water surface elevation data from tidal gages. This model simulated the flow conditions within the model domain based on the forcing conditions provided (e.g., wind, wave, tides). Then, the sediment transport model, SEDZLJ, was set up using measured data from the SEDFLUME study and Particle Imaging Camera System (PICS) analysis (Smith & Friedrichs, 2015). This model simulated the deposition

of sediment onto the bed and resuspension of sediment from the bed to the water column. Lastly, the contaminant transport model was set up using calculated chemical partitioning coefficients and measured PCB concentrations. The EFDC model calculated the concentration of PCBs sorbed to particulate matter, bound to dissolved organic carbon, and in the freely dissolved phase (all together the total PCB concentration). The PCB contaminant transport model was calibrated "using the time series of predicted PCB dissolved in the water column and particulate-bound PCB concentrations and outputting these results from the respective model grid cell (certain cells represented a physical location where PCB concentrations were measured during the data collection phase). To make adjustments based on the first calibration run, the diffusion coefficient responsible for determining the flux of PCBs moving from the bed to the water column was adjusted until the model gave the best overall agreement with the measured and predicted dissolved and particulate PCB concentrations. After the modeling system (hydrodynamics, sediment, and contaminant transport) was calibrated, the selected 30-year simulations of post-remediation conditions in the harbor for three different scenarios were performed" (Hayter et al. 2014). The conclusion from this report indicated that there was very slow change in PCB concentrations in the harbor over the 30-year period due to the low energy environment inside the harbor and the slow diffusive flux rate of PCBs. The results from this study were conclusive and used to better understand the health risk associated with the PCBs in the harbor. The current research aims to achieve a similar outcome and by developing a three-tier model that can be used to evaluate the effectiveness of selected remediation alternatives and provide additional information to decision makers seeking to clean up contaminated sites to protect the environment and human health.

PHREEQC APPLICATION

PHREEQC was used in a study completed in Mexico that determined arsenic speciation in a drinking water aquifer. In the study, “hydrogeochemical modeling for speciation of arsenic was carried out with PHREEQC version 3.0 software based on the databaseWATEQ4F.dat. The program implemented the ion-associated theory of aqueous solutions and Debye–Hückel expressions to execute various aqueous geochemical calculations” (Ortiz-Letechipia et al., 2022). The objective of this study was to compare the arsenic species present in the aquifer from 2015 and 2020 to select a remediation technique that would be suitable to clean up the groundwater and protect drinking water for the surrounding community. First, groundwater samples were collected each year and electrical conductivity, pH, dissolved oxygen, and total dissolved solids were measured. The electrical conductivity and pH are needed to describe the aquifer in terms of oxidizing or reducing conditions. Depending on the redox state, different inorganic arsenic species will be present (reducing conditions – As(3) dominates; oxidized conditions – As(5) dominates). These data were used to set up the solutions in PHREEQC. After running the program, the results showed that As(5) dominated this region of the Calera aquifer based on the analyzed samples, while that of As(3) was found in very small quantities in both years. The study concluded, “arsenic speciation allows us to know the behavior and mobilization of this element in groundwater for different purposes, for example, to find an adequate remediation method that helps to improve the quality of life of the population, while providing safe drinking water” (Ortiz-Letechipia et al., 2022). Similar to the work completed by Ortiz-Letechipia et al., (2022) groundwater samples collected from 16 monitoring wells near the Vineland Superfund site were used to set up the batch solutions in PHREEQC to calculate the distribution of As(3) and As(5). The fraction of arsenic species present at each monitoring well can be used to evaluate the toxicity at each well. Understanding how toxic the site is can help decision makers select appropriate remediation techniques and prioritize where remediation should begin within a contaminated site in order to protect people and the

environment. The current research demonstrates how PHREEQC can be applied to calculated arsenic speciation and discuss future potential uses for this tool in conjunction with a contaminant transport model like EFDC+.

PREVIOUS STUDIES CONDUCTED AT VINELAND CHEMICAL SUPERFUND SITE

This next section describes previous studies performed at Vineland Chemical Superfund site to gain background information about this site.

In 2004, researchers from Columbia University, NY conducted a study at the Vineland Chemical Superfund site (Keimowitz et al., 2005). This study sampled the porewater and sediments from BWB and measured stream discharges to evaluate factors driving arsenic mobilization. Two cross-channel transects were taken at each location to measure the stream velocity. Surface water was returned to the laboratory for high resolution inductively coupled plasma mass spectrometry (ICPMS) analysis. ICPMS quantified sulfur, manganese, iron, and arsenic in stream water, porewater, and all sequential sediment extraction steps. The research found that the groundwater discharge to the BWB is the most plausible source of arsenic and the main pathway for arsenic to be carried downstream to the Maurice River and Union Lake. Overland transport, effluent from the pump and treat plant, and remobilization of sediment-bound arsenic in BWB were all ruled out based on site-specific knowledge and collected stream data. This research was important for documenting the arsenic mobilization at the bed of the BWB tributary and confirming the plausibility of groundwater discharge re-contaminating the site. This study confirmed that groundwater moves vertically upward into BWB, a gaining stream. This study was completed in 2005 and during the following year, OU3's floodplain soils were excavated and treated to clean up the soil and reduce arsenic contamination surrounding BWB above the water table. Despite this cleanup effort and the ongoing pump and treat system responsible for treating the contaminated groundwater, more recent sampling events have indicated that arsenic persists in the area including downgradient of the Superfund site. The current research uses subsurface sediment and groundwater

data collected in 2022-2023 (USACE, 2023) to set up the PHREEQC model and characterize the level of toxicity at the 16 monitoring wells along the BWB.

A study conducted by Lockheed Martin SERAS (2015) on behalf of the USEPA Environmental Response Team in Edison, NJ occurred from 2012 to 2014 to assess the extent of contamination, assess arsenic transport through the Maurice River system, and evaluate high-use areas along Maurice River and Union Lake for potential threats to human and ecological systems. During the three-year period (referred to as the 3-year study), natural river flushing was used to allow the submerged, arsenic-contaminated sediments in the Maurice River to be transported by natural processes (Lockheed Martin SERAS, 2015). During this study, flow rates were measured at transects throughout the Maurice River system and these discharge data were used to calibrate the EFDC+ hydrodynamic model (Figure 5). A SEDFLUME analysis was conducted in 2013 (Sea Engineering Inc., 2013) to characterize the sediment erosion properties and physical characteristics of the lake and river sediments. These data were used to set up the input files for the sediment transport model. Finally, sampling locations were selected along the Maurice River and Union Lake to measure concentrations of total arsenic in surficial and subsurface sediments and surface water (Figure 6). These data were used to set up and calibrate the contaminant transport model.

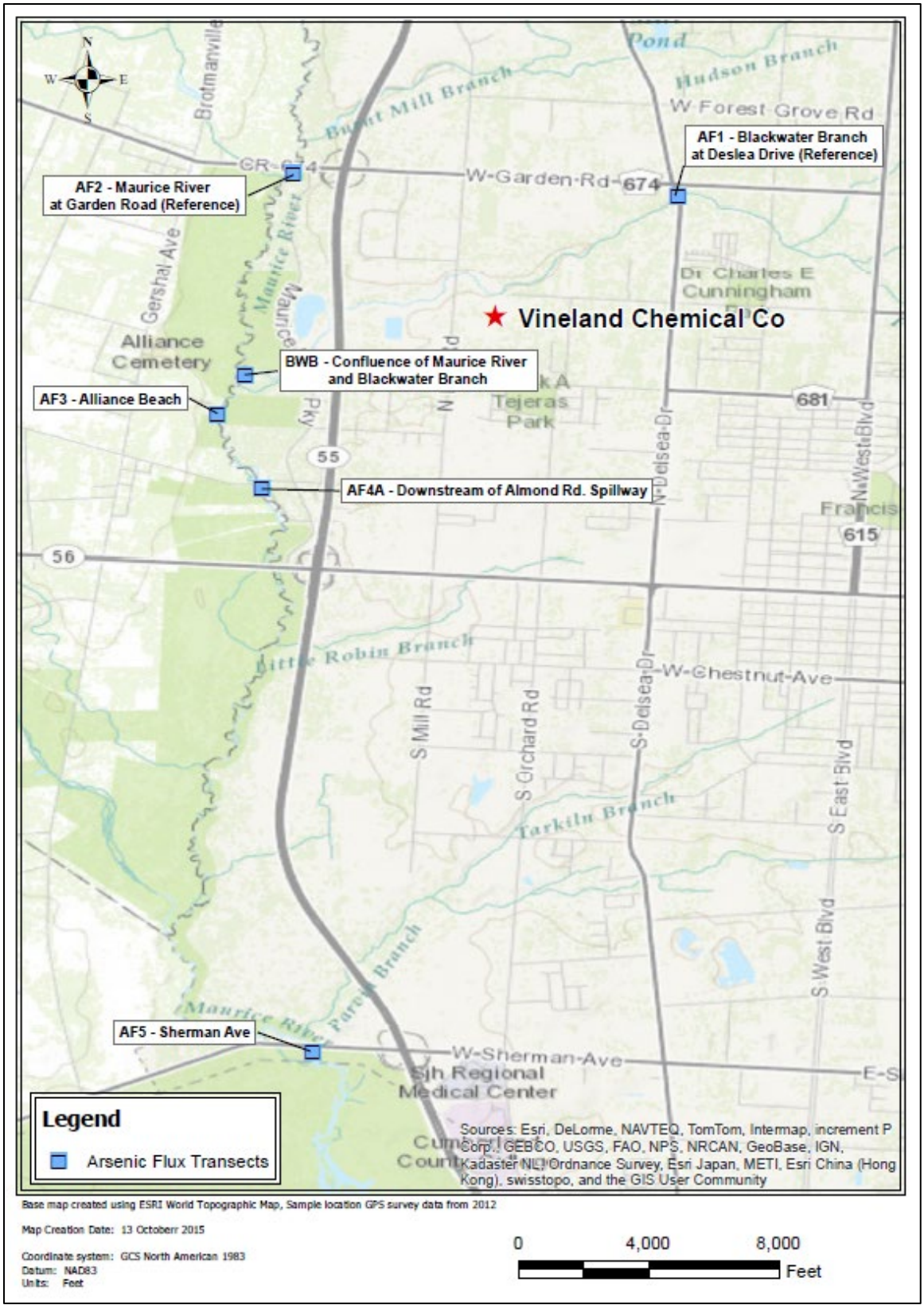

Figure 5: 3-Year Study Discharge Measurement Locations (Lockheed Martin SERAS, 2015)

Figure 6: 3-Year Study Sampling Locations Analyzed for Arsenic (Lockheed Martin SERAS, 2015)

III. MULTI-TIER MODELING SYSTEM & PHREEQC DESCRIPTION

The models included in the three-tier modeling system (Figure 1) and the PHREEQC model are described in more detail in this section. Also included is a description of the setup of these models to represent the Maurice River System.

HYDROLOGICAL SIMULATION PROGRAM FORTRAN MODEL

Hydrological Simulation Program – FORTRAN (HSPF) is a mathematical model developed by Donigian Jr. et al. (1995) with support from the USEPA and USGS to simulate hydrologic and water quality processes in natural and manmade water systems. The model is commonly used in the fields of hydrology and water quality management and is recognized as one of the most comprehensive watershed hydrology and water quality models available (RESPEC 2024). HSPF can simulate continuous, dynamic, or steady-state behavior of both hydrologic/hydraulic and water quality processes in a watershed, with an integrated linkage of surface, soil, and stream processes (Duda, Hummel, Donigian Jr., & Imhoff, 2012).

HSPF is paired with the Better Assessment Science Integrating Point and Nonpoint Sources (BASINS) program that was developed by the USEPA (USEPA, 2019). BASINS is a multipurpose environmental analysis system designed to help perform watershed and water quality-based studies. The BASINS environment facilitates data acquisition, data management, geographic data processing, and watershed delineation. BASINS provides model-specific data input formatting capabilities and can parameterize and launch models including HSPF (USEPA, 2019). BASINS is used to delineate the HSPF watershed and provide characteristics using the BASINS databases (e.g., meteorological or land cover). For this study, only the portion of the Maurice River watershed upstream of Union Lake is used in HSPF because the EFDC+ model domain ends at the Union Lake Spillway. The extent of the watershed model domain used for HSPF is shown in Figure 7. Next, the BASINS watershed delineation tool was used to

delineate subbasins (smaller watershed basins within the original watershed) which were categorized by land type from the Nation Land Cover Database (NLCD) 2019 database into four land uses: wetland/water, urban, forest, and cropland. After setting up the subbasins, each subbasin was assigned a reach (RCH) corresponding to a particular section of river or tributary within the watershed. The reaches (RCHRES) used to represent the Maurice River and tributaries are shown in Figure 8. After the watershed was set up, BASINS generated a HSPF project folder which included the HSPF user control input (UCI) file. Using a text editor, the UCI file parameters were adjusted to represent the Maurice River watershed.

There are three main modules used to parameterize the watershed in the UCI file: pervious land (PERLND), impervious land (IMPLND), and water bodies (RCHRES). PERLND accounts for the surface runoff, interflow, and baseflow. IMPLND accounts for surface runoff from impervious surfaces. Both PERLND and IMPLND hydrology parameters were specified based on characteristics of the Maurice River watershed. Examples of these parameters include infiltration rate, overland slope, soil moisture storage, and evapotranspiration. Values for the PERLND and IMPLND parameters came from a previous BASINS/HSPF modeling study for the Upper Maurice River Watershed (Shirinian-Orlando & Uchrin, 2012). Flow routing parameters include length and depth of RCHRES and are automatically specified by BASINS for each RCHRES. HSPF simulated the flow from specified RCHRES including the runoff from PERLND and IMPLND land surfaces.

Once the UCI file was setup, HSPF ran from 2012 to 2015 and calculated the flow rate exiting each RCH. The UCI file parameters were adjusted and HSPF simulations were repeated until HSPF simulated discharges closely matched measured discharge data. For this study, the calibration point is located at Almond Road in Norma, NJ where USGS gage 01411500 is located. The results from HSPF are presented in Chapter 4, including a discussion regarding the determination of the upstream boundary discharge for EFDC+ at the Maurice River at Garden Road.

Figure 7: Portion of Maurice River Watershed used in HSPF Model Shown in Red.

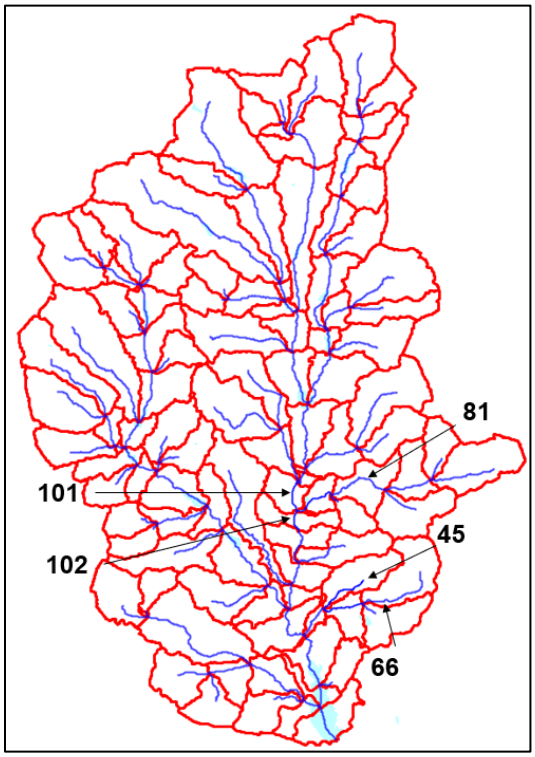

Figure 8: BASINS Subbasins (red) and RCHRES (blue). RCH 101 = Garden Road, RCH 102 = Almond Road, RCH 81 = BWB, RCH 45 = Tarkiln, RCH 66 = Parvin

CLEMSON UNIVERSITY HYDROGRAPH

Developed by Dr. Lawrence Murdoch, a Clemson University Environmental Engineering and Earth Sciences faculty member, CU Hydrograph is a Microsoft Excel program that executes a hydrograph separation analysis to separate baseflow and storm flow and determine groundwater discharge into surface water. The selected hydrograph separation method for this program comes from the Wallingford Institute of Hydrology (Wesselink & Gustard, 1992) which calculates the baseflow using the following procedure:

1. Divide the daily flow into five-day non-overlapping blocks and calculate the minimum for each of these blocks.
2. Determine turning points of the five-day minimum values.
3. Connect the turning point to give the separated base flow line.

The water table in the coastal plains of New Jersey is shallow and it was appropriate to include groundwater discharge into the Maurice River in this modeling study because the Maurice River is a gaining reach. Measured discharge data from the USGS gage 01411500 and historic precipitation data for Vineland, NJ were used to setup the worksheet for 10 years (2007 to 2017). Using 10 years was important to capture enough high flow events and recession events to estimate a representative baseflow. Figure 9 shows the hydrograph generated by CU Hydrograph.

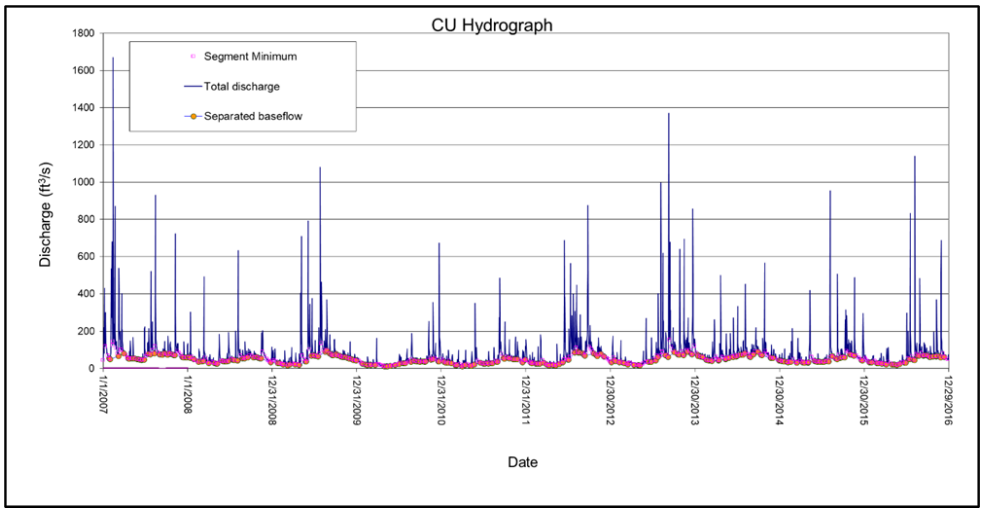

Figure 9: Hydrograph from CU Hydrograph

Monthly averages for	10.01 Years					
	Precip	ET	Runoff	Recharge	Baseflow	Stormflow
Jan	0.2512	0.2044	0.0889	0.0071	0.0492	0.0397
Feb	0.2790	0.1704	0.1097	0.0483	0.0494	0.0603
March	0.3002	0.1989	0.0921	0.0601	0.0509	0.0413
April	0.3866	0.2700	0.0880	0.0830	0.0543	0.0337
May	0.3433	0.1700	0.1179	0.1261	0.0707	0.0472
June	0.3147	0.0728	0.1768	0.1576	0.0925	0.0843
July	0.4318	0.2030	0.1870	0.1462	0.1045	0.0825
Aug	0.3125	0.1323	0.1800	0.1145	0.1142	0.0658
Sept	0.2985	0.1656	0.1571	0.0862	0.1103	0.0467
Oct	0.2945	0.2045	0.1294	0.0546	0.0940	0.0354
Nov	0.2842	0.2107	0.1224	0.0249	0.0737	0.0487
Dec	0.2616	0.2266	0.0787	0.0174	0.0610	0.0176

Figure 10: Monthly Average of Groundwater Discharge (Baseflow) from 2007 to 2017

The Excel worksheet calculated the baseflow and storm flow for the Maurice River watershed area. After the program ran, the monthly flux of baseflow, recharge, and evapotranspiration was written out into a separate Excel worksheet. Figure 10 shows the average monthly flux reported for the entire watershed (384 square miles) [994.6 square km] discharging into the Maurice River over 10 years. To convert the output to a volumetric rate per segment of the Maurice River, six of the watershed subbasins from BASINS were used to divide the entire watershed into six smaller reaches. Then, the volumetric baseflow rate (m^3/s) for each of the six segments of the Maurice River was calculated. The baseflow calculated for each segment of the Maurice River was divided by the number of grid cells representing each segment of the Maurice River and copied into the groundwater time series input file,

GWSER.inp, for the EFDC+ hydrodynamic model. The method used to calculate the groundwater discharge per segment of the Maurice River assumed that the subbasin areas from BASINS are representative of the ground watershed area and could be used to divide the total baseflow originally calculated in the Excel worksheet.

MODFLOW is a USGS developed three-Dimensional finite difference groundwater model that simulates steady and non-steady flow in an irregularly shaped flow system in which aquifer layers can be confined, unconfined, or a combination of confined and unconfined (Harbaugh 2005). In 2013, a MODFLOW model was developed and calibrated for this Superfund site by the U.S. Army Corps of Engineers Philadelphia District which included calculating the groundwater discharge to the Maurice River. Unfortunately, the groundwater discharge results could not be interpreted correctly to use in the GWSER.inp input file. The MODFLOW model did not represent the groundwater discharge from 2012 to 2015, thus it could not provide groundwater discharge rates during this modeling period. MODFLOW provided the average groundwater discharge into the Maurice River every 500 feet [152.4 m] but there was no date/time associated with these values. Instead, CU Hydrograph was used and compared to the results from the MODFLOW model as shown in Table 1. The comparison showed that the calculated flows from both models and the flow per length of the Maurice River from each model were comparable. The results from CU Hydrograph were used in the GWSER.inp file to represent the groundwater discharging into the Maurice River for the EFDC+ hydrodynamic model. The average groundwater discharge rate was two orders of magnitude smaller than the average discharge of the upstream discharge for the Maurice River indicating that the groundwater discharge was not a significant driving force for the hydrodynamic model. The results from CU Hydrograph were considered acceptable and used as input for the EFDC+ hydrodynamic model.

In future studies, the MODFLOW model should be reevaluated and used to estimate the groundwater discharge into the Maurice River from 2012-2015. This existing model was developed using

site-specific data from Vineland Chemical Superfund Site and should provide a more realistic groundwater discharge time series because it was developed using measured groundwater data to represent the Maurice River ground watershed.

Table 1: CU Hydrograph and MODFLOW Groundwater Discharge Comparison

	CU Hydrograph	MODFLOW
Length of Maurice River (m)	365.5	152.4
Flow (m^3/s)	0.0385	0.0396
Flow per Length of Maurice River ($m^3/s/m$)	1.05E-04	2.60E-04

ENVIRONMENTAL FLUID DYNAMICS CODE +

EFDC+ is an updated version of EFDC (Hamrick, 1992) developed by Dynamic Solutions International, LLC and operates within the EFDC+ Explorer Modeling System (EEMS) graphical user interface. EEMS provides a broad range of pre-processing and post-processing tools to assist in developing, calibrating, and analyzing EFDC+ models (DSI, LLC, 2024). EFDC+ is an open source, surface water modeling system capable of simulating one, two and/or three-dimensional hydrodynamics and water column constituent transport. Before running EFDC+, the model domain was set up using a curvilinear grid which contained 32,383 curved cells as opposed to Cartesian cells that use straight lines. Figure 4 shows the curvilinear grid cells used to represent the model domain. A curvilinear grid allows for better representation of the physical space. Coarser grid cells represent the floodplains and portions of Union Lake while finer grid cells are used to represent the Maurice River and tributaries. The range in cell sizes allows for increased resolution in areas of the model domain that require more detail or have complex geometries. The grid cells representing the Almond Road Weir and Union Lake Spillway were assigned to be a sharp crested weir and broad crested weir, respectively. Each weir required a crest elevation, width of weir, and coefficient of discharge which were provided by USGS (2024). Once the grid was developed, elevation data from 2019 provided by the state of New Jersey (NJDEP, 2019) were

assigned to each grid cell in the model domain. This dataset did not include bathymetric data which is important for representing the bottom elevation in the river, tributaries, and lake. However, this is the only available elevation data currently. To estimate the bottom elevation, the elevation (vertical NAVD88 Datum in meters) of the hydraulic structures (Almond Road Weir and Union Lake Spillway), the elevation of the riverbanks, and available stream cross-section profiles were used to interpolate bottom elevations for each waterbody. Although there were no river or lake bottom elevation data, the elevation of the Union Lake Dam and Spillway controlled the water surface elevation in the lake and lower Maurice River. The model domain with the 2019 elevation dataset is shown in Figure 11. After developing the model grid and adding the interpolated elevation data, the three modeling components of EFDC+ can be set up and run. Each component of EFDC+ is described below.

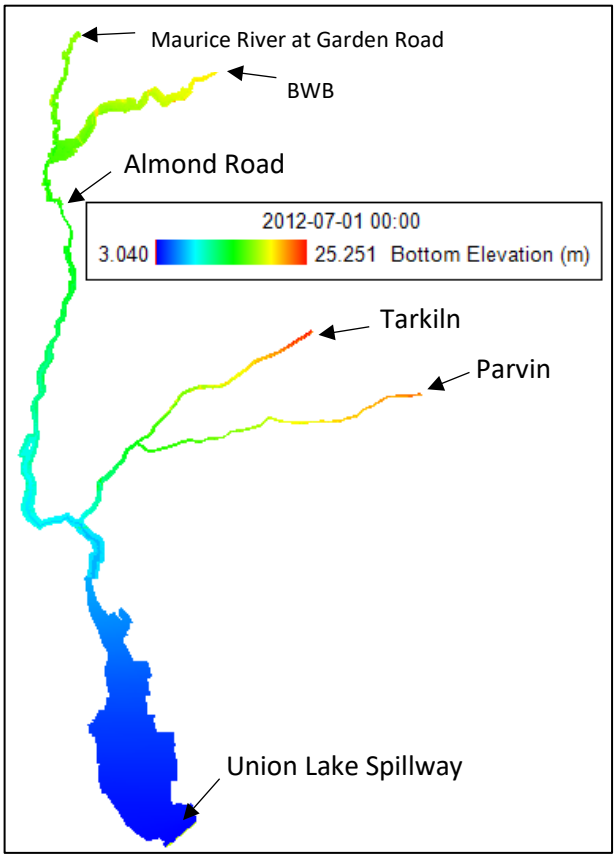

Figure 11: EFDC+ Model Domain with NJDEP 2019 Elevation Data

HYDRODYNAMIC MODEL

The EFDC+ hydrodynamic model is a finite-difference numerical model that uses a staggered grid to solve the equations of motion and achieve second-order accuracy both in space and time. Details of the finite difference numerical schemes used in the EFDC model are given in DSI, LLC (2020).

The EFDC+ hydrodynamic model operates based on the laws of conservation for mass, momentum, and energy of the flow. In EFDC+ it is assumed that the ambient environmental flows have horizontal length scales which are greater than the vertical length scales. EFDC+ uses a curvilinear coordinate system in the horizontal direction and a sigma transformation for the vertical direction.

EFDC+ solves the 3D, vertically hydrostatic, free surface, turbulence averaged equations of motion for an incompressible, variable density fluid which are shown below. Equation 2-1 represents the conservation of mass which states that the time rate of change of fluid in the control volume is equal to the net flux of fluid leaving the control volume. Equation 2-2 represents the conservation of linear momentum in the x direction in which the time rate of change of linear momentum in the x-direction is equal to the sum of forcings acting on the control volume in the x-direction. The forcings include the water surface slope, pressure gradient due to varying pressure across a surface, internal losses due to turbulence, bottom friction, wind-stress at the surface, Coriolis force, and momentum sources/sinks. Equation 2-3 represents the conservation of linear momentum in the y-direction. Equation 2-4 is the hydrostatic pressure equation. Equations 2-1 to 2-4 are the equations of motion transformed so that the horizontal coordinates, x and y, are curvilinear and orthogonal.

$$\frac{\partial(m\varepsilon)}{\partial t}+\frac{\partial(m_y Hu)}{\partial x}+\frac{\partial(m_x Hv)}{\partial y}+\frac{\partial(mw)}{\partial z}=0 \qquad (2\text{-}1)$$

$$\frac{\partial(mHu)}{\partial t}+\frac{\partial(m_xHuu)}{\partial x}+\frac{\partial(m_xHvu)}{\partial y}+\frac{\partial(mwu)}{\partial z}-\left(mf+v\frac{\partial(m_y)}{\partial x}-u\frac{\partial m_x}{\partial y}\right)Hv$$

$$=m_yH\frac{\partial(g\varepsilon+p)}{\partial x}-m_y\left(\frac{\partial H}{\partial x}-z\frac{\partial H}{\partial x}\right)\frac{\partial p}{\partial z}+\frac{\partial(mH^{-1}A_v\frac{\partial u}{\partial z})}{\partial z}+Q_u$$

(2-2)

$$\frac{\partial(mHv)}{\partial t}+\frac{\partial\left(m_yHuv\right)}{\partial x}+\frac{\partial(m_xHvv)}{\partial y}+\frac{\partial(mwv)}{\partial z}+\left(mf+v\frac{\partial(m_y)}{\partial x}+u\frac{\partial m_x}{\partial y}\right)Hu$$

$$=m_xH\frac{\partial(g\varepsilon+p)}{\partial y}-m_x\left(\frac{\partial H}{\partial y}-z\frac{\partial H}{\partial y}\right)\frac{\partial p}{\partial z}+\frac{\partial(mH^{-1}A_v\frac{\partial v}{\partial z})}{\partial z}+Q_v$$

(2-3)

$$\frac{\partial p}{\partial z}=\frac{gH(\rho-\rho_o)}{\rho_o}=gHb$$

(2-4)

In each of these equations, ε is the water surface elevation, u and v are the mean horizontal velocity components in (x, y) coordinates; m_x and m_y are the square roots of the diagonal components of the metric tensor, and $m = m_x m_y$ is the Jacobian or square root of the metric tensor determinant; *p* is the pressure in excess of the reference pressure given by $\frac{\rho_o gH(1-z)}{\rho_o}$, where ρ_o is the reference density; *f* is the Coriolis parameter for latitudinal variation, A_v is the vertical turbulent viscosity; A_b is the vertical turbulent diffusivity. The buoyancy, *b,* in Equation 2-4 is the normalized deviation of density from the reference value. $H = h + \zeta$ is the total depth. Q_u and Q_v are the source/sink terms for the horizontal momentum in the x and y directions, respectively. The sigma transformation for the vertical direction is used to maintain the same number of vertical layers when the model is run in three dimensions regardless of water depth and is given by:

$$z=\frac{(z^*+h)}{(\zeta+h)}$$

(2-5)

where z* is the physical vertical coordinate, and h and ζ are the depth below and the displacement about the undisturbed physical vertical coordinate origin, z* = 0, respectively. For this research, two-dimensional model is set up because there is no stratification of the vertical layer, and a single, depth-averaged vertical layer is used.

Equations 2-1 to 2-4 are solved in EFDC+ using turbulence-averaged values because instantaneous velocities and concentrations cannot be solved for turbulent flows. The instantaneous values are averaged over the time scale of turbulence to yield turbulence averaged values to generate a solution. The equations of motion (2-1 to 2-4) use the Boussinesq approximation for variable density. In each of these equations the change in density is assumed to be very small, essentially negligible; however, the varying density is accounted for in the terms that include gravity.

At the bottom of the vertical boundary (sediment bed) represented by a subscript of 1, the bed shear stresses are computed using near bed velocity components (u_1, v_1) as:

$$(\tau_{bx}, \tau_{by}) = c_b \sqrt{u_1^2 + v_1^2}(u_1, v_1) \qquad (2\text{-}6)$$

where the bottom drag coefficient, $c_b = (\frac{\kappa}{\ln(\frac{\Delta_1}{2z_o})})^2$, where k is the von Karman constant, Δ_1 is the dimensionless thickness of the bottom layer, $z_o = z_o^*/H$ is the dimensionless roughness height, and z_o^* is roughness height in meters. At the surface of the vertical boundary (water surface), the shear stresses are computed using the *u, v* components of the wind velocity (u_w, v_w) above the water surface (usually measured at 10 m above the surface) and are given as:

$$(\tau_{sx}, \tau_{sy}) = c_s \sqrt{u_w^2 + v_w^2}(u_w, v_w) \qquad (2\text{-}7)$$

where $c_s = 0.001 \frac{\rho_a}{\rho_w}(0.8 + 0.065)\sqrt{u_w^2 + v_w^2}$ and ρ_a and ρ_w are the air and water densities, respectively.

SEDIMENT TRANSPORT MODEL

The SEDZLJ sediment transport model is used in this modeling study (Jones and Lick, 2001; James et al., 2010). Details regarding the sediment transport model equations come from DSI, LLC (2020). SEDZLJ is dynamically linked to EFDC+ in that the hydrodynamics and sediment transport modules run simultaneously during each time step. The sediment bed in the Maurice River contains a mixture of cohesive and non-cohesive sediments (very fine sand). When the sediment bed consists of mainly cohesive or a mixture of cohesive and non-cohesive size sediments, SEDZLJ uses results obtained from a SEDFLUME analysis. SEDFLUME is a straight, closed conduit, rectangular cross-section flume in which detailed measurements of critical shear stress of erosion and erosion rate as a function of sediment depth are made using sediment cores collected at the site to be modeled (McNeil, Taylor, & Lick, 1996). SEDZLJ uses the results from SEDFLUME testing to determine the erosion rate of the top layer of the sediment bed. This modeling study's SEDFLUME testing was conducted in August of 2013 (Sea Engineering Inc., 2013). The erosion rate for various applied shear stresses was approximated using the power law regression equation given by:

$$E = A\tau^n \qquad (2\text{-}8)$$

where τ is the applied bed shear stress, and *A* and *n* are empirical coefficients that are functions of the sediment bulk density. For each depth interval, the measured erosion rates and applied shear stresses were used to determine the values of *A* and *n* that provide a best fit power law curve to the data at each interval. Regression analysis was then used to estimate the critical shear stress (the applied shear stress at which incipient motion of sediment begins) for each interval (Sea Engineering Inc., 2013).

Sediment samples were collected throughout the model domain and analyzed for grain size distribution. Based on the analysis, eight discrete sediment size classes (3, 15, 75, 150, 300, 600, 900, 1200 µm) were chosen to represent the sediment bed across the study area. The smallest class size, 3

µm, represents flocs, the 15 µm size represents bed aggregates, and the remaining classes represent non-cohesive sediments (>63 µm). Each of the eight sediment size classes represents the mean diameter within that size range. SEDZLJ simulates the transport of each of the sediment classes to determine the suspended sediment concentration for each size class in the water column layer in each grid cell at each time step. The transport equation solved in EFDC+ for suspended sediment load having a mass per unit volume concentration *C*, is:

$$\frac{\partial(m_x m_y HC)}{\partial t} + \frac{\partial(m_y HuC)}{\partial x} + \frac{\partial(m_x HvC)}{\partial y} + \frac{\partial(m_x m_y w_{sc} C)}{\partial z}$$

$$= \frac{\partial}{\partial_x}\left(\frac{m_y}{m_x} HK_H \frac{\partial C}{\partial x}\right) + \frac{\partial}{\partial_y}\left(\frac{m_x}{m_y} HK_H \frac{\partial C}{\partial y}\right) + \frac{\partial}{\partial_z}\left(m_x m_y \frac{K_v}{H} \frac{\partial C}{\partial z}\right) + Q_c$$

(2-9)

where K_v and K_H are the vertical and horizontal turbulent diffusion coefficients, respectively; w_{sc} is a positive settling velocity when C represents the mass concentration of suspended sediment; and Q_c represents external sources (due to erosion) or sinks (due to deposition). For sediment, C = S_j , where S_j represents the concentration of the jth sediment class. in this modeling study, j = 1,8. The transport equation uses a high-order upwind difference solution scheme for the advection terms (Hamrick, 2007). The advection scheme is set up to minimize numerical diffusion; however, a small amount of horizontal diffusion remains inherent in the numerical scheme. Thus, the horizontal diffusion terms in Equation 2-9 are omitted by setting K_H equal to zero. Equation 2-9 represents the conservation of mass for the non-conservative constituent, S_j . The time rate of change of suspended sediment concentration in the model domain is equal to the net flux of suspended sediment concentration exiting the model domain.

The settling of cohesive sediments is a complex process that is difficult to measure without a device like a PICS. The settling of flocculated cohesive sediment depends on the aggregation and disaggregation of flocs which is influenced by turbulence (i.e., internal shear), differential settling, and Brownian motion, surface composition of a particle, and interparticle bonding strength of the floc. There

was no PICs study completed at this site, but the mean settling velocities for cohesive size sediments (3 µm and 15 µm) measured from the PICS study for the New Bedford Harbor Superfund site (Hayter et al. 2014) were also applied to this study. The settling velocities for non-cohesive sediments are calculated in SEDZLJ using the following equation by Cheng (1997).

$$w_s = \frac{\mu}{d}(\sqrt{25 + 1.2d_*^2} - 5)^{\frac{3}{2}}$$

(2-10)

where μ = dynamic viscosity of water; d = sediment diameter; and d^* = non-dimensional particle diameter given by:

$$d_* = d[\left(\frac{\rho_s}{\rho_w} - 1\right) g/v^2]^{\frac{1}{3}}$$

(2-11)

where ρ_w = water density, ρ_s = sediment particle density, g = acceleration due to gravity, and v = kinematic fluid viscosity. Cheng's formula is based on measured settling speeds of real sediments with irregular shapes. Compared to Stokes' Law which assumes a perfectly spherical shape, the settling speeds from Cheng's formula are lower because irregular shaped particles have a greater hydrodynamic resistance to settling compared to spherical particles.

SEDZLJ uses Van Rijn (1984) approach to simulate bedload transport. The equation representing the conservation of mass for the concentration of non-cohesive sediment moving as bedload is given by:

$$\frac{\partial(\delta_{bl} C_b)}{\partial t} = \frac{\partial q_{b,x}}{\partial x} + \frac{\partial q_{b,y}}{\partial y} + Q_b$$

(2-12)

where δ_{bl} = bedload thickness; C_b = bedload concentration; $q_{b,x}$ and $q_{b,y}$ = x and y components of the bedload sediment flux, respectively; and Q_b = sediment flux from the bed. Van Rijn (1984) gives the following equation for the thickness of the layer in which bedload is occurring:

$$\delta_{bl} = 0.3dd_*^{0.7}(\Delta\tau)^{0.5}$$

(2-13)

where $\Delta\tau = \tau_b - \tau_{ce}$; τ_b = bed shear stress, and τ_{ce} = critical shear stress for erosion. The bedload fluxes in the x- and y- directions are given by:

$$q_{b,x} = \delta_{bl} u_{b,x} C_b$$

(2-14)

$$q_{b,y} = \delta_{bl} u_{b,y} C_b$$

(2-15)

where $u_{b,x}$ and $u_{b,y}$ = x- and y- components of the bedload velocity, u_b, which van Rijn (1984) gave as

$$u_b = 1.5\tau_*^{0.6}[\left(\frac{\rho_s}{\rho_w} - 1\right) gd]^{0.5}$$

(2-16)

with the dimensionless parameter τ^* given as:

$$\tau_* = \frac{\tau_b - \tau_{ce}}{\tau_{ce}}$$

(2-17)

The x- and y-components of u_b are calculated as the ratios of *u* and *v* to the total hydrodynamic velocity times u_b, respectively. The sediment flux from the bed due to bedload, Q_b, is equal to:

$$Q_b = E_b - D_b$$

(2-18)

$$E_b = P_e W_s C_e$$

(2-19)

$$D_b = P_d W_s C_b$$

(2-20)

where E_b is the erosion of sediment into bedload, and D_b is the deposition of sediment from bedload onto the sediment bed, P_e is the probability of erosion, P_d is the probability of deposition, W_s is the

particle settling speed, C_e is the steady state equilibrium concentration of sediment in bedload, and C_b is the bedload concentration.

The erosion and deposition of each of the sediment size classes in Equation 2-9, and the subsequent change in the composition and thickness of the sediment bed in each grid cell are calculated by SEDZLJ at each time step. An active layer formulation is used to describe sediment bed interactions during simultaneous erosion and deposition. The active layer facilitates coarsening during the bed armoring process. Figure 12 shows the simulated sediment transport processes in SEDZLJ where U = near bed flow velocity, δ_{bl} = thickness of layer in which bedload occurs, U_{bl} = average bedload transport velocity, D_{bl} = sediment deposition rate for the sediment being transported as bedload, E_{bl} = sediment erosion rate for the sediment being transported as bedload, E_{sus} = sediment erosion rate for the sediment that is eroded and entrained into suspension, and D_{sus} = sediment deposition rate for suspended sediment.

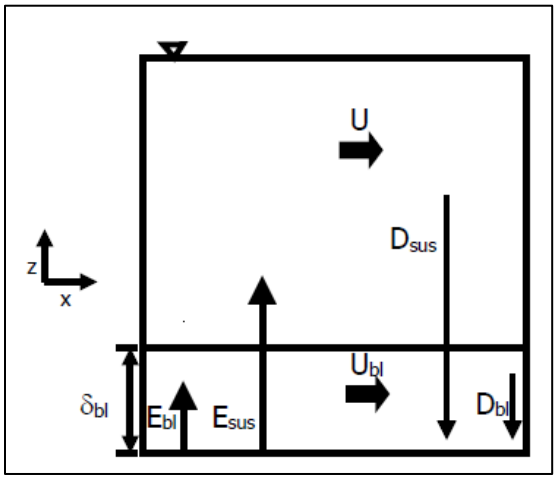

Figure 12: Sediment Transport Processes Simulated in SEDZLJ (Hayter et al. 2014)

To represent the processes of erosion and deposition, the sediment bed in SEDZLJ was divided into seven layers, some of which are used to represent the existing sediment bed and others that are used to represent new bed layers that form due to deposition during model simulations. Figure 13

shows a diagram of this multiple bed layer structure. The first layer is the active layer representing the exchange between the bed and water columns, the second layer is the new deposits layer, layers 3-6 are representative of the sediment cores collected during the SEDFLUME testing, and layer 7 is the non-erodible bottom bed layer. At the start of a sediment transport model run, layer 3 represents the top bed layer.

SEDZLJ can represent multiple size sediment classes in the sediment bed which is necessary to simulate coarsening and subsequent armoring of the surficial sediment bed surface during high flow events. As states previously, eight sediment size classes are being used in this model. Bed armoring is a process that occurs during high flow events that decreases the sediment bed erosion rate for cohesive and non-cohesive sediments. During a high flow event, a bed composed of multiple size sediment classes tends to erode the finer particles faster than the coarser particles. Each sediment class has different erosion rates, and this creates a fine layer at the surface sediment bed, known as the active layer, where finer particles are scarce and coarser particles are abundant. As a result, bed armoring can occur, where the active layer consists mainly of coarser particles. The multi-layered bed model in SEDZLJ accounts for the changing composition of the active layer and the exchange of sediment through this layer. The changing composition of all bed layers is due to changes in the percentage (by mass) of the eight size classes mainly in the top bed layers due to erosion and deposition of different size classes in each grid cell. The thickness of the active layer is normally calculated as a time varying function of the mean sediment particle diameter in the active layer, the critical shear stress for resuspension corresponding to the mean particle diameter, and the bed shear stress. Figure 14 shows a diagram of the active layer at the top of the multi-bed layer model used in SEDZLJ.

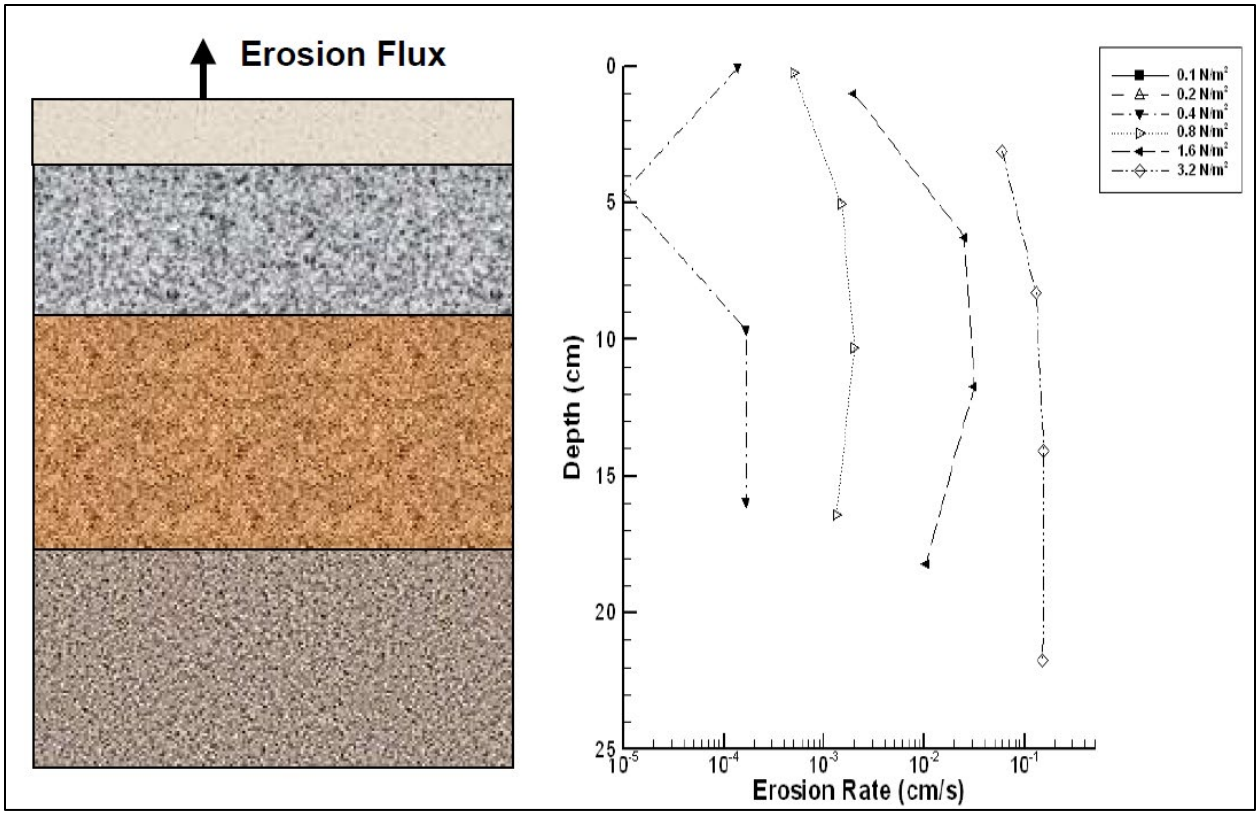

Figure 13: Multi-Bed Layer Model Used in SEDZLJ (Hayter et al. 2014)

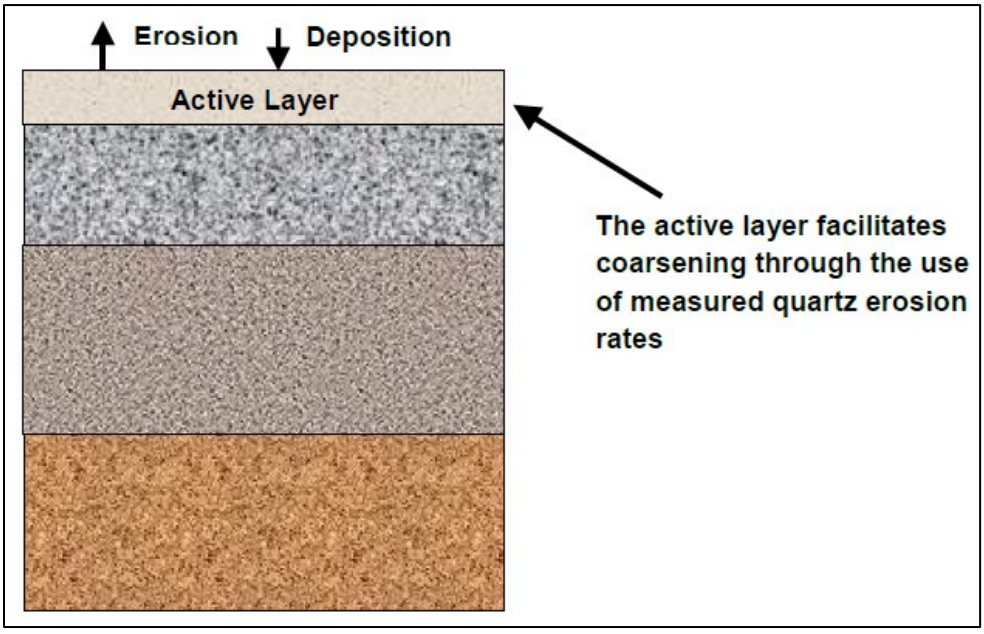

Figure 14: Diagram of Active Layer Used in SEDZLJ (Hayter et al. 2014)

CONTAMINANT TRANSPORT MODEL

The contaminant transport model in EFDC+ uses a three-phase equilibrium partitioning model to simulate the transport of arsenic. A three-phase partitioning model explicitly accounts for the freely dissolved contaminant, the contaminant bound to dissolved organic carbon (DOC), and the contaminant bound to particulate organic matter (POC), or sediments. The sum of the contaminant concentrations of all three phases is equal to the total concentration. Details regarding the contaminant transport model equations come from DSI, LLC (2020).

While the actual time it takes to reach complete equilibrium can be very long, it is often assumed that equilibrium between the dissolved and particulate phases occurs over a time scale of only a few hours to a day (Jepsen et al., 1995). This is the basis of the equilibrium partitioning assumption that is often used in contaminant transport modeling.

Both dissolved and particulate-bound arsenic are advected by the flow of the Maurice River, tributaries, and groundwater flow into these gaining reaches. Adsorbed arsenic is transported with sediment as the latter are moved as a result of bed load, suspended load, deposition, and resuspension as simulated by the sediment transport model. There is also a vertical diffusive flux of arsenic that occurs in proportion to the gradient between the dissolved arsenic concentration in the water column and that in the pore water. As sediment is eroded, arsenic in the porewater is released from the bed into the water column. This diffusive flux is due to molecular diffusion and bioturbation. The diffusive flux coefficient value for this model was set to 1E-10 m^2/s (Hayter et al. 2014). The transport equation representing the conservation of mass for the freely dissolved chemical is:

$$\partial_t(m_x m_y H C_w) + \partial_x(m_y H u C_w) + \partial_y(m_x H v C_w) + \partial_z(m_x m_y w C_w)$$

$$= \partial_z\left(m_x m_y \frac{A_b}{H}\partial_z C_w\right) + m_x m_y H\left(\sum_i K_{dS}^i S^i \chi_S^i + \sum_j K_{dD}^j D^j \chi_D^j\right)$$

$$- m_x m_y H(\sum_i K_{aS}^i S^i(\psi_w \frac{C_w}{\varphi})(\hat{\chi}_S^i - \chi_S^i) + \sum_j K_{aD}^j D^j(\psi_w \frac{C_w}{\varphi})(\hat{\chi}_D^j - \chi_D^j) + \gamma C_w$$

(2-21)

where C_w is the mass of freely dissolved contaminant per unit total volume, C_S is the mass of contaminant sorbed to sediment class i per mass of sediment, C_D is the mass of contaminant sorbed to dissolved material *j* per unit mass of dissolved material, φ is the porosity, ψ_w is the fraction of the freely dissolved contaminant available for sorption, K_a is the adsorption rate, K_d is the desorption rate, and γ is a net linearized decay rate coefficient. Since equilibrium partitioning is assumed, the adsorption and desorption rates are both equal to zero. The sorption kinetics are based on the Langmuir isotherm (Chapra, 1997) with $\hat{\chi}$ denoting the saturation adsorbed mass per carrier mass. The solids and dissolved material (i.e., DOC) concentrations, *S* and *D*, respectively, are defined as mass per unit total volume. The index *j* is the number of contaminants, and the index *i* is the number of classes of solids, i.e., organic particulate matter and inorganic sediment. The initial concentrations of DOC and POC in the water column was set to 1 mg/L and 0 mg/L, respectively. The initial concentration of DOC and POC in the sediment bed was set to 10 mg/L and 5 mg/L, respectively. There were no available measured data for this site, but literature values for coastal plain rivers such as the Maurice River had values within this range for both DOC and POC (USGS, 1976). The transport equation for the contaminant adsorbed to DOC is:

$$\partial_t\left(m_x m_y H D^j \chi_D^j\right) + \partial_x\left(m_y H u D^j \chi_D^j\right) + \partial_y\left(m_x H v D^j \chi_D^j\right) + \partial_z\left(m_x m_y w D^j \chi_D^j\right)$$
$$= \partial_z\left(m_x m_y \frac{A_b}{H} \partial_z (D^j \chi_D^j)\right) + m_x m_y H\left(K_{sD}^j D^j\right)\left(\psi_w \frac{C_w}{\varphi}\right)\left(\hat{\chi}_D^j - \chi_D^j\right) - m_x m_y H(K_{dD}^j$$
$$+ \gamma)(D^j \chi_D^j)$$

(2-22)

The transport equation for the contaminant adsorbed to suspended solids is:

$$\partial_t\left(m_x m_y H S^i \chi_S^i\right) + \partial_x\left(m_y H u S^i \chi_S^i\right) + \partial_y\left(m_x H v S^i \chi_S^i\right) + \partial_z\left(m_x m_y w S^i \chi_S^i\right) + \partial_z\left(m_x m_y w_S^i S^i \chi_S^i\right)$$
$$= \partial_z\left(m_x m_y \frac{A_b}{H} \partial_z (S^i \chi_S^i)\right) + m_x m_y H\left(K_{aS}^i S^i\right)\left(\psi_w \frac{C_w}{\varphi}\right)\left(\hat{\chi}_S^i - \chi_S^i\right) - m_x m_y H(K_{dS}^i$$
$$+ \gamma)(S^i \chi_S^i)$$

(2-23)

The concentrations (in units of sorbed mass per unit total volume) of chemicals adsorbed to DOC and solids, C_D and C_S, respectively, are defined as:

$$C_D^j = D^j \chi_D^j$$

(2-24)

$$C_S^i = S^i \chi_S^i$$

(2-25)

Introducing Equations 2-24 and 2-25 into Equations 2-21 to 2-23 gives:

$$\partial_t\left(m_x m_y H C_w\right) + \partial_x\left(m_y H u C_w\right) + \partial_y\left(m_x H v C_w\right) + \partial_z\left(m_x m_y w C_w\right)$$
$$= \partial_z\left(m_x m_y \frac{A_b}{H} \partial_z C_w\right) + m_x m_y H\left(\sum_i K_{dS}^i C_S^i + \sum_j K_{dD}^j C_D^j\right)$$
$$- m_x m_y H(\sum_i K_{aS}^i S^i (\psi_w \frac{C_w}{\varphi})(\hat{\chi}_S^i - \chi_S^i) + \sum_j K_{aD}^j D^j (\psi_w \frac{C_w}{\varphi})(\hat{\chi}_D^j - \chi_D^j) + \gamma C_w$$

(2-26)

$$\partial_t\left(m_x m_y H C_D^j\right) + \partial_x\left(m_y H u C_D^j\right) + \partial_y\left(m_x H v C_D^j\right) + \partial_z\left(m_x m_y w C_D^j\right)$$

$$= \partial_z\left(m_x m_y \frac{A_b}{H}\partial_z\left(C_D^j\right)\right) + m_x m_y H\left(K_{sD}^j D^j\right)\left(\psi_w \frac{C_w}{\varphi}\right)\left(\hat{\chi}_D^j - \chi_D^j\right) - m_x m_y H\left(K_{dD}^j + \gamma\right)\left(C_D^j\right)$$

(2-27)

$$\partial_t\left(m_x m_y H C_S^i\right) + \partial_x\left(m_y H u C_S^i\right) + \partial_y\left(m_x H v C_S^i\right) + \partial_z\left(m_x m_y w C_S^i\right) + \partial_z\left(m_x m_y w_S^i C_S^i\right)$$

$$= \partial_z\left(m_x m_y \frac{A_b}{H}\partial_z\left(C_S^i\right)\right) + m_x m_y H\left(K_{aS}^i S^i\right)\left(\psi_w \frac{C_w}{\varphi}\right)\left(\hat{\chi}_S^i - \chi_S^i\right) - m_x m_y H\left(K_{dS}^i + \gamma\right)\left(C_S^i\right)$$

(2-28)

The EFDC sorbed contaminant transport formulation currently assumes equilibrium partitioning with the adsorption and desorption terms in Equations 2-27 and 2-28 being equal, such that:

$$\left(K_{sD}^j D^j\right)\left(\psi_w \frac{C_w}{\varphi}\right)\left(\hat{\chi}_D^j - \chi_D^j\right) = K_{dD}^j C_D^j$$

(2-29)

$$\left(K_{aD}^i S^i\right)\left(\psi_w \frac{C_w}{\varphi}\right)\left(\hat{\chi}_S^i - \chi_S^i\right) = K_{dS}^i C_S^i$$

(2-30)

Solving Equations 2-29 and 2-30 for the ratio of C_D and C_S to C_w gives:

$$\frac{C_D^j}{C_w} = \frac{f_D^j}{f_w} = P_D^j \frac{D^j}{\varphi}$$

(2-31)

$$\frac{C_S^i}{C_w} = \frac{f_S^i}{f_w} = P_S^i \frac{S^i}{\varphi}$$

(2-32)

where *P* is the partition coefficient. Using literature values from (Allison & Allison, 2005), the water column and sediment bed partition coefficients were set to 2.5 (L/mg). The partition coefficients for DOC in the water column and sediment bed were 0.025 and 0.25, respectively. The partition coefficients for POC in the water column and sediment bed were 0.025 and 2.5, respectively. With the relationship between the mass fractions expressed as:

$$f_w + \sum_i f_S^i + \sum_j f_D^j = 1$$

(2-33)

the expressions for these three fractions are given by:

$$f_w = \frac{C_w}{C} = \frac{\varphi}{\varphi + \sum_i P_S^i S^i + \sum_j P_D^j D^j}$$

$$f_D^j = \frac{C_D^j}{C} = \frac{P_D^j D^j}{\varphi + \sum_i P_S^i S^i + \sum_j P_D^j D^j}$$

$$f_S^i = \frac{C_S^i}{C} = \frac{P_S^i S^i}{\varphi + \sum_i P_S^i S^i + \sum_j P_D^j D^j}$$

(2-34)

Adding Equations 2-26, 2-27, and 2-28, and using the equilibrium partitioning relationships given by Equations 2-29 and 2-30 gives the following transport equation for the total contaminant concentration:

$$\partial_t(m_x m_y HC) + \frac{1}{m_x m_y}\partial_x(m_y HuC) + \frac{1}{m_x m_y}\partial_y(m_x HvC) + \partial_z(m_x m_y wC) - \partial_z\left(m_x m_y \sum_i w_S^i f_S^i C\right)$$
$$= \partial_z\left(m_x m_y \frac{A_b}{H}\partial_z C\right) - m_x m_y H\gamma C$$

(2-35)

Equation 2-35 is solved for *C*, and then the concentrations for the three phases are solved for using the relationships given by Equation 2-34. During the 3-year study (Lockheed Martin SERAS, 2015), sediment and surface water samples were collected and analyzed for total and dissolved arsenic. In the Spring of 2022, sediment and surface water samples were collected from the Tarkiln and Parvin Branches and analyzed for total and dissolved arsenic under the Former Kil-Tone OU4 Remedial Investigation (HDR OBG, 2022). These datasets were used to specify the initial conditions (e.g., spatially varying concentrations of the total arsenic in sediment bed) for the sediment bed and water column concentration of arsenic. The initial concentration of total arsenic in the water column was set to 1.3 μg/L based on the average value of arsenic measured in the surface waters throughout the model domain. The boundary condition for the surface water and sediment arsenic concentrations included downstream of the Maurice River confluence with BWB, the tributaries, and Union Lake. Table 2 shows the initial concentrations of arsenic in the sediment bed which were determined using the average value of arsenic measured in the sediment throughout the model domain. Figure 6 shows the measured sampling locations for surface water and sediment sampling collected during the 3-year study from 2012-2015.

Table 2: Initial Sediment Bed Arsenic Concentration throughout Model Domain

Location	BWB	Alliance Beach	Almond Road	BA Beach	Parvin	Tarkiln	Union Lake
As Concentration in Sediment Bed (mg/kg)	35	25	19	4.5	2 (Upper) 6.5 (Lower)	9	130 (upper) 200 (lower)

PHREEQC

PHREEQC is a computer program developed by the USGS for simulation of chemical reactions and transport processes in natural or polluted water, in laboratory experiments, or in industrial processes. PHREEQC can be used as a speciation program to calculate saturation indices, the distribution of aqueous

species, and the density and specific conductance of a specified solution composition. PHREEQC uses the chemical composition of a water sample (i.e., solution) to calculate the aqueous species produced from the reaction between the solution and the minerals present in the subsurface. In PHREEQC, the surfaces command is used to calculate the amount of contaminant (i.e., arsenic) that sorbs to the surface mineral (Parkhurst & Appelo, 2013).

The purpose of using PHREEQC for this research was to demonstrate the model's ability to predict the species of arsenic, As(3) and As(5), present in the subsurface and groundwater that feed into BWB, a gaining reach. The results from PHREEQC can be used to understand the level of toxicity at the Vineland Chemical Superfund site and determine if current and future remediation solutions are appropriate based on which arsenic species are present in the groundwater and surface water. Figure 15 shows a simplified conceptual model of the exchange between the sorption and dissolution of arsenic and iron. Arsenic in the groundwater will sorb to sediments if enough mineralized iron is present to provide sorption sites for arsenic to attach to. As the iron precipitates, arsenic co-precipitates and if there is dissolution of iron, the sorbed arsenic will desorb and return to its aqueous phase.

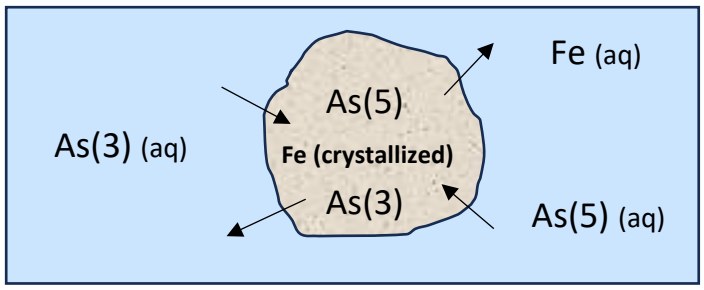

Figure 15: Conceptual Model: Exchange between Aqueous and Sorbed Arsenic and Iron

For this research, groundwater data and available mineralogy data were used to set up the PHREEQC input file and run several batch reactions, each representing a monitoring well along BWB. The input file is constructed in the Windows graphical user interface using groundwater data collected from the BWB from 2023. The structure of the input file consists of various command blocks that represent

the contaminant of concern, the chemical properties of the water and/or soil, and how the contaminant of concern behaves in the system. Details regarding the setup of each command block can be found in (Parkhurst & Appelo, 2013). The following commands are used in the arsenic speciation model for the BWB.

SURFACE_MASTER_SPECIES: This command block is used to define the correspondence between surface binding-site names and surface master species. Normally, this data block is included in the database file and only additions and modifications are included in the input file. The surface species for hydrous aluminum oxide were added to the input file for this research.

PHASES: This command adds new minerals to the EQUILIBRIUM_PHASES command if any minerals are missing from the model. This command fixed the pH and redox potential for this research.

SURFACE_SPECIES: This command creates new surface complexes (sorbed species). Additional surface complexes for aluminum, arsenic, and iron were added to the Minteq.v4 database. Below are the reactions used in PHREEQC to calculate the arsenic sorbed to aluminum and iron (Dzombak & Morel, 1990). Each reaction shows the reactants on the left-hand side and the products on the right-hand side. The 's' indicates a strong site, and the 'w' indicates a weak site for sorption. Below the reaction is the equilibrium constant, log(K). This indicates the direction of the reaction and whether the products or the reactants will dominate at equilibrium.

```
Hao_sOH = Hao_sOH
       log_k  0.0

Hao_sOH + H+ = Hao_sOH2+
          log_k  7.17

Hao_sOH = Hao_sO- + H+
         log_k  -11.18

Hao_sOH + Fe+2 = Hao_sOFe+ + H+
             log_k -3.77

Hao_sOH + H3AsO4 = Hao_sH2AsO4 + H2O
            log_k 5.83
```

```
Hao_sOH + H3AsO4 = Hao_sHAsO4- + H2O + H+
               log_k 0.68

 Hao_sOH + H3AsO4 = Hao_sOHAsO4-3 + 3H+
             log_k -14.72

  Hao_sOH + H3AsO4 = Hao_sH2AsO4 + H2O
               log_k 5.83

Hao_sOH + H3AsO4 = Hao_sHAsO4- + H2O + H+
               log_k 0.68

 Hao_sOH + H3AsO4 = Hao_sOHAsO4-3 + 3H+
             log_k -14.72

  Hfo_sOH + H3AsO3 = Hfo_sH2AsO3 + H2O
               log_k 5.41

  Hfo_wOH + H3AsO3 = Hfo_wH2AsO3 + H2O
               log_k 5.41

  Hfo_sOH + H3AsO4 = Hfo_sH2AsO4 + H2O
               log_k 8.61

  Hfo_wOH + H3AsO4 = Hfo_wH2AsO4 + H2O
               log_k 8.61

Hfo_sOH + H3AsO4 = Hfo_sHAsO4- + H2O + H+
               log_k 2.81

Hfo_wOH + H3AsO4 = Hfo_wHAsO4- + H2O + H+
               log_k 2.81

 Hfo_sOH + H3AsO4 = Hfo_sOHAsO4-3 + 3H+
             log_k -10.12

 Hfo_wOH + H3AsO4 = Hfo_wOHAsO4-3 + 3H+
             log_k -10.12
```

SURFACE: This command defines the amount and composition of each surface in a surface assemblage. The sites per mole and surface area of kaolinite and goethite were added to represent each weak and strong bonding site that arsenic may sorb to as well as the presence of each mineral. There was no available database for kaolinite adsorption reactions. Instead, the database containing gibbsite mineralogy data were used to approximate kaolinite's surface area and site per mole parameters (Karamalidis & Dzombak, 2010). The assumption in this model is that the kaolinite clay edge sites (containing one silica tetrahedral sheet and one alumina octahedral sheet) will behave as aluminol

(AlOH) sites in gibbsite. This assumption has been used in other surface complexation models where gibbsite was used as a surrogate for montmorillonite (Powell, Kersting, Zavarin, & Zhao, 2008). This assumption allows the gibbsite constants to be used to predict the arsenic sorption to kaolinite. Table 3 shows the mineralogy data used to set up the surfaces command.

Table 3: Surface Characteristics for Goethite and Kaolinite

	Goethite	Kaolinite
Sites per Mole	0.2 (weak) 0.002 (strong)	.0033 (strong)
Surface Area (m^2)	22	10.05

SOLUTION: This command is used to define the solutions, or the composition of the groundwater sample, for each batch reaction. Groundwater data from 2023 collected at 16 wells surrounding BWB near the Vineland Chemical Superfund site were used to create each solution (Figure 16). The general trend for groundwater movement is upward and westward towards BWB. These 16 wells were selected due to their proximity to BWB and because the appropriate measured data were available at these locations. Each batch reaction solution contains groundwater data from shallow (S) and mid-depth (M) wells. This dataset includes major ion concentrations, aqueous arsenic and iron concentrations, pH, and redox potential.

EQUILIBRIUM_PHASES: This command defines the amounts of an assemblage of pure phases that can react reversibly with the aqueous phase. When then phases are brought in contact with an aqueous solution, each phase will dissolve or precipitate to achieve equilibrium. Goethite and kaolinite were added to this command block to react with each SOLUTION and were linked to the moles of available surface sites for sorption reactions through the SURFACE_SPECIES command.

SELECTED_OUTPUT: this command is used to specify the data shown in the output file which can be read out as an excel file.

After the command blocks described above are filled in with the available data, PHREEQC runs and provides the fraction of each arsenic species present based on the geochemical conditions specified in the input file.

Figure 16: Wells Along BWB Used in PHREEQC

Due to limited available geochemistry data, additional correction factors were used. For example, to determine the moles of mineral surface area per pore volume in the aquifer, the given percent of goethite and kaolinite was converted to moles of each mineral per 100 grams of soil. The bulk density of the soil and the porosity were used to determine a solid to liquid ratio that could be used to approximate the moles of mineral per pore volume. Additionally, a correction factor of 0.1 was used because the groundwater can only flow through pore spaces, not the bulk materials of the aquifer. It is also important to recognize that the PHREEQC model includes goethite and kaolinite as the only adsorbing surfaces present in the aquifer. These are the dominant minerals present in the aquifer, but a more sophisticated model could be developed to represent the aquifer if more mineralogy data were available.

After setting up the input file, PHREEQC was run to calculate the fraction of sorbed and aqueous arsenic and the fraction of aqueous As(3) and As(5) present in the groundwater. The results are shown in Table 4 and Table 5. Using the recorded pH and redox potential for each sample, an Eh-pH, or Pourbaix, diagram was generated to show the stable species of arsenic present in each well sample. The species above the red horizontal line are As(5) and the species below the line are As(3). Most of the samples had an Eh of 0.025 or greater within a pH range of 3 to 7.

Table 4: Fraction of Arsenic Sorbed and Fraction of Arsenic in Aqueous Form

Fraction Aqueous As	Fraction of Sorbed As
0.01	0.99

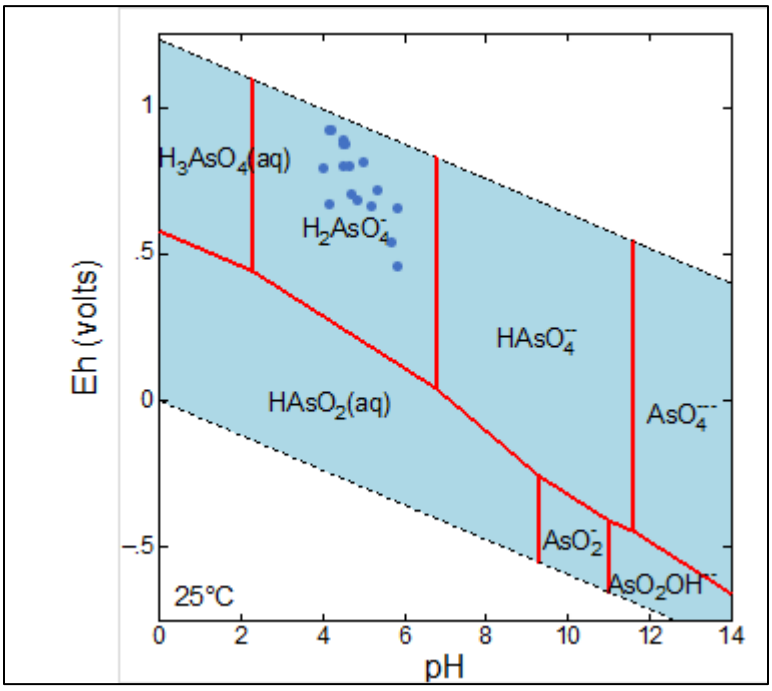

Figure 17: Pourbaix Diagram Generated Using Geochemist Workbench and the llnl.dat Database

The results from PHREEQC were able to simulate the speciation of arsenic present surrounding the Vineland Chemical Superfund site near BWB based on the measured water chemistry. Figure 17 shows that the dominant species of arsenic in all samples is predicted to be arsenate, H_2ASO4^-. Almost

all the arsenic is sorbed to the goethite and kaolinite in the form arsenate. The fraction of aqueous As(3) and As(5) in the groundwater is shown below in Table 5. The fraction of aqueous arsenic present is very small, and the distribution of aqueous arsenic is dominantly As(5). The measured data collected did not include arsenic speciation data to verify the results from PHREEQC. However, in a 5-year Review Report for the Vineland Chemical Company Superfund site, the report indicated, "As an aside, arsenic speciation shows that overall arsenate is the dominant form of arsenic; however, there are periods where arsenite is the dominant form of arsenic in process water" (USEPA, 2011). Depending on the pH, redox potential, and availability of iron, the speciation of arsenic may change. Based on the measured pH and redox potential the samples collected and used for this study were in an oxidized environment indicating arsenate was the dominant form of arsenic. Because the arsenate is tightly bound to the iron in the sediments and soil, the contaminant is relatively stabilized (sorbed to mineralized iron) and less likely to move into BWB and further downstream posing a greater threat to humans and the environment. Therefore, the human health risk is reduced because the arsenic is dominantly sorbed to the sediment and soils and not as available in the aqueous phase. This is likely due to the presence of goethite in the aquifer which is a well-known iron mineral which can sorb arsenic (Mamindy-Pajany 2009).

Table 5: Average As(3) and As(5) Fraction in Aqueous Form

Fraction As(3),	Fraction As(5),
0.01	0.99

Based on the results from PHREEQC and the current knowledge of the site, this tool could be useful for future studies at this site and others to determine which species may be present and/or dominant. It's important to note that the aquifer is not homogenous or isotropic, meaning that there

are different geochemical conditions beneath the surface and the results from PHREEQC cannot be applied site wide to the entire model domain because the speciation of arsenic is dependent on the aquifer environment. The results from this study demonstrated how PHREEQC can be used to provide the distribution of arsenic species at the specific wells used in the study.

In future contaminant transport modeling studies, a tool like PHREEQC could be used in conjunction with a contaminant transport model like EFDC+ to predict distribution of species present at selected grid cells within the model domain. For example, if there was a hot spot (localized area of high arsenic concentration) of arsenic contamination in a river, and two remediation alternatives were being simulated in EFDC+, the simulated total arsenic concentration output from EFDC+ could be used in PHREEQC to predict the species of arsenic and concentrations present at that hotspot in each of the remediation alternatives. Of course, the geochemical data for that hotspot would need to be collected in advance, but the output from EFDC+ in conjunction with PHREEQC could predict if As(3) or As(5) is more dominant and therefore, predict how harmful the hotspot area could be for the local ecosystem and human health.

IV. MODEL CALIBRATION

This chapter discusses the procedures used to calibrate each model.

HYDROLOGICAL SIMULATION PROGRAM FORTRAN MODEL

The HSPF model simulated the runoff and upstream discharge at the BWB, Tarkiln Branch, and Parvin Branch. The simulated upstream discharge for the Maurice River at Garden Road was not representative of the actual flow in the Maurice River, and thus could not be used for the upstream boundary conditions for EFDC+. This is further discussed below.

After running the HSPF model from 2012 to 2015, the discharge time series plots were generated to determine which IMPLND and PERLND parameters in the UCI file would be adjusted. The simulated discharge flows for the Maurice River and tributaries were compared to measured discharge data from USGS Gage 01411500 at Almond Road and the five discharge measurements from the 3-year study (Figure 5). The results from this model carry uncertainty due to the limited measured data available for calibration of the flow in the tributaries and downstream of Almond Road of the Maurice River.

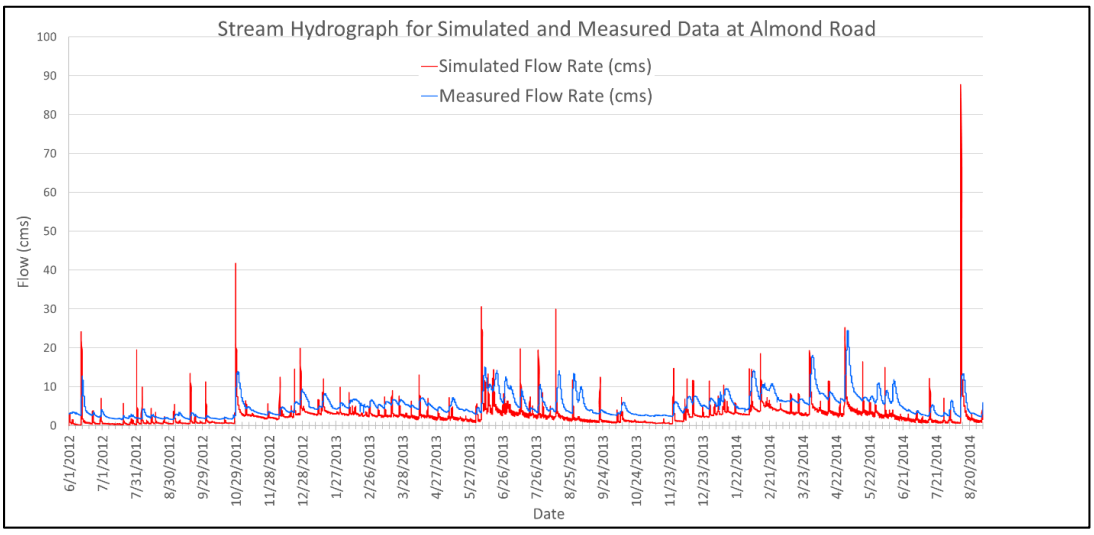

Figure 18: HSPF Simulated and Measured Discharge at Almond Road with High Precipitation

The initial parameters set in the UCI file produced a simulated flow rate at Almond Road that followed the same general trend as the measured flow at the USGS gage, but the base flow was lower and some of the storm events overestimated storm flow (Figure 18). After discussing these initial results with a senior-level HSPF modeler (A. Mishra. Personal Communication. October 2022), the first adjustment to the UCI file was adding a multiplier value of 0.6 to the potential evapotranspiration (PET). This reduced the calculated PET and provided a larger base flow by restricting the ability for water to evaporate into the air. After consulting HSPF guidance and reviewing technical notes, the BASINS meteorological (MET) data were further reviewed. Climate and weather data were generated in BASINS from the North American Land Data Assimilation System (NLDAS) database. After reviewing NLDAS precipitation data, it was discovered that some of the precipitation values may have been over predicted. Historical weather data were reviewed to confirm if the precipitation patterns in the NLDAS database were consistent with historical precipitation data from 2012-2015. In particular, the HSPF model predicted the occurrence of a large storm event in August of 2014 whereas the observed weather data indicated that no significant storms occurred during that period. It is possible that the database could have inaccurate precipitation data, or the weather device malfunctioned. To verify if the MET station was overestimating the rainfall during August 2014, the precipitation data were decreased by half, and the model was rerun. The results showed a decreased peak flow rate, one that was more consistent with the observed rainfall and discharge from the USGS gage at Almond Road. HSPF was not able to fully represent this complex watershed and with limited data available to construct the model, the output from HSPF became more challenging to calibrate; however, the important goal was to simulate discharge in the Maurice River and tributaries. After further consultation (A. Mishra. Personal Communication. June 2023), the precipitation data were adjusted by reducing values by 30-50% depending on the storm event. Figure 19 shows the simulated discharge after running the model with the adjusted precipitation data. The extreme peak flows are drastically reduced over the three years

while the baseflow continues to follow the trends of the measured flow rate from June 2012 to January 2015. However, in the first six months, the HSPF model greatly underestimated the flow in the Maurice River at Almond Road. Parameters in the UCI file like infiltration and evapotranspiration were decreased to see if the model would respond and provide a higher baseflow, but the results did not change. The initial volume of water in the HSPF reach was also increased, but the model results did not change.

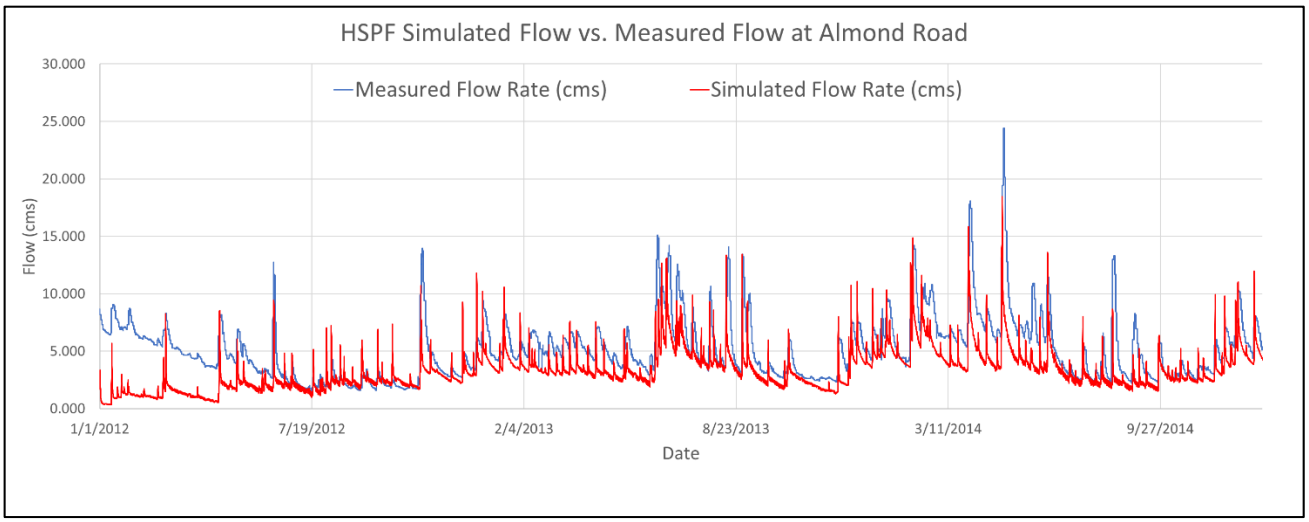

Figure 19: HSPF Simulated and Measured Flow Rates at Almond Road with Reduced Precipitation

Figure 20 shows the simulated upstream boundary discharge for the Maurice River at Garden Road plotted with the simulated and measured discharge of the Maurice River at Almond Road. As expected, the flow rate in the Maurice River at the upstream boundary is less than the flow at Almond Road because it does not include the flow from BWB. The flow at the upstream boundary (Garden Road) was measured once during each of the following months: July 2012, October 2012, May 2013, October 2013, and July 2014 (see Figure 21). At the five instances when the flow was measured, there is reasonable agreement between the measured and simulated flows, but because the discharge measurements were not continuous there was more uncertainty in using these data to calibrate HSPF. It is important to use reliable discharge data to represent boundary conditions, especially for the Maurice River because it is the main hydraulic conduit in the model domain and the sediment and contaminant

transport models will not be accurate if the hydrodynamic component of EFDC+ misrepresents true flow conditions. It was concluded that the HSPF discharge for the upstream boundary of the Maurice River should not be used and instead, the measured discharge from the USGS gage at Almond Road was modified and used to represent the EFDC+ upstream boundary discharge for the Maurice River. The USGS gage at Almond Road provides discharge data which includes the flow from BWB. The simulated flow out of the BWB during the 3-year study was about 4% of the flow in the Maurice River at Almond Road. In order to use the USGS gage to represent the upstream discharge for the Maurice River at Garden Road, the measured flow data were reduced by 4% to avoid overestimating the flow at the upstream boundary at Garden Road.

The HSPF simulated discharge for the BWB is shown in Figure 22. The BWB flow rate was measured five times throughout the 3-year study. As seen in this figure, the HSPF simulated flow is consistent with the measured flow rates from the five dates when flow was recorded. There was no available continuous discharge measured along the Blackwater Branch, so this was the best available data to verify if the simulated flow was representative of the BWB. This output from HSPF was deemed satisfactory and therefore used to represent the upstream boundary discharge for BWB in the EFDC+ hydrodynamic model.

There were no measured discharge data for the Tarkiln and Parvin Branches. Figure 23 shows the HSPF simulated flows for the Tarkiln and Parvin Branches. Qualitatively, the flow rates from both tributaries behaved as expected because the flows were consistent with site knowledge. The Tarkiln is an intermittent stream with smaller flows than the Parvin. The simulated flows were used to represent the upstream boundary discharge and surface runoff into the Parvin and Tarkiln Branches, but future modeling studies should measure flow continuously over at least one year to use for calibration of the EFDC+ hydrodynamic model.

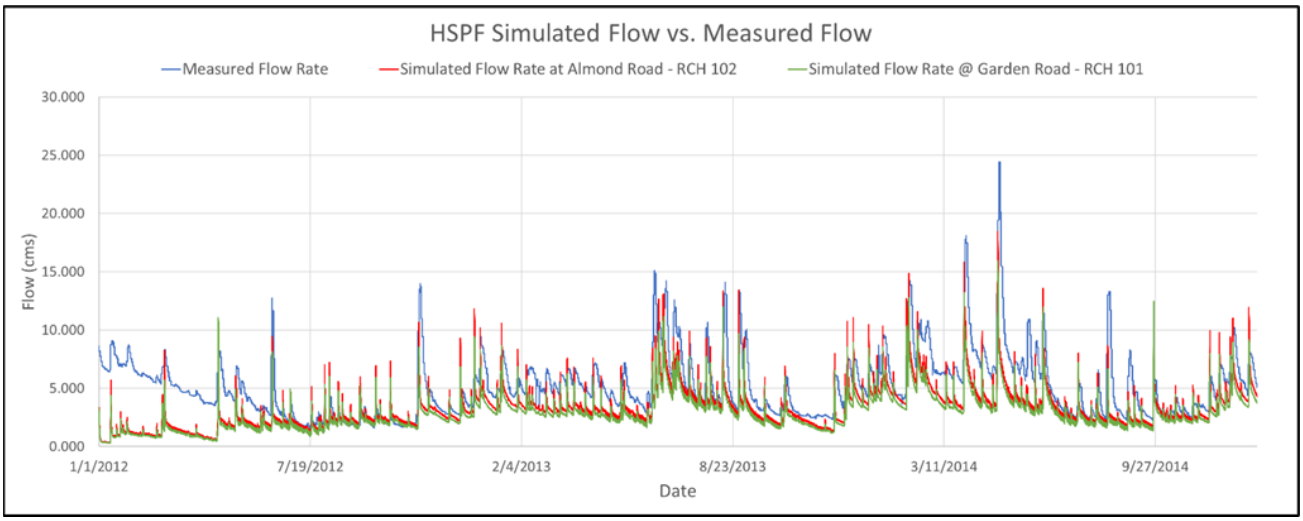

Figure 20: HSPF Simulated Flows at Garden Road (101) and Almond Road (RCH 102)

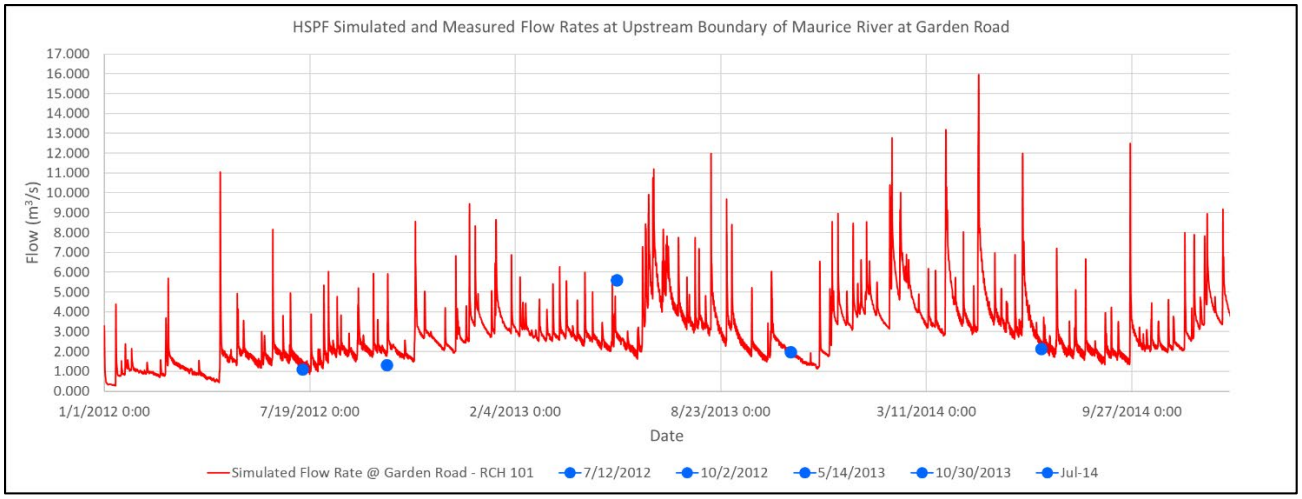

Figure 21: Simulated and Measured Flow at Upstream Boundary of Maurice River at Garden Road

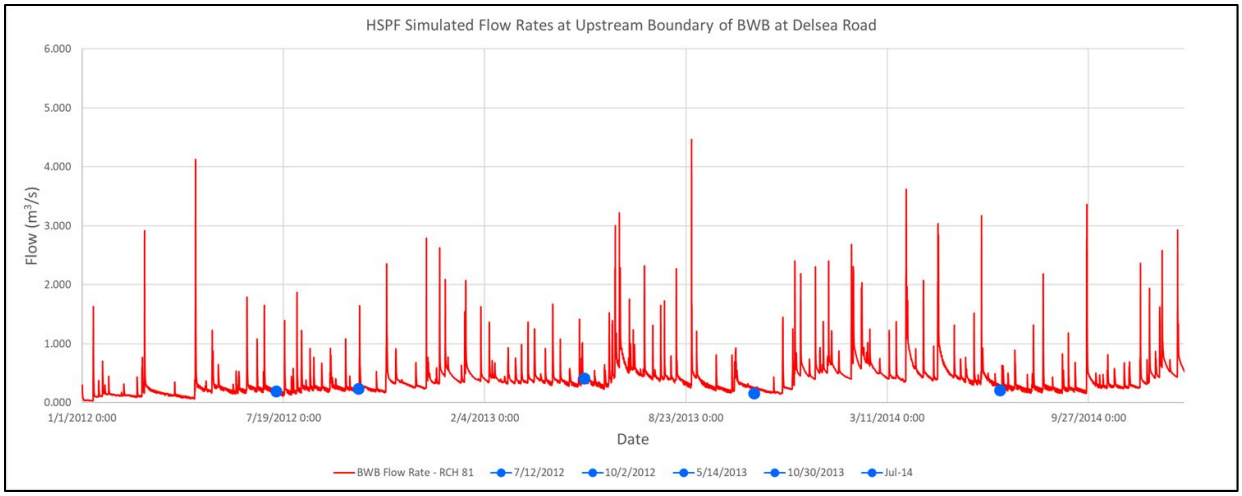

Figure 22: Simulated Flow and Measured Flow at Upstream Boundary of BWB

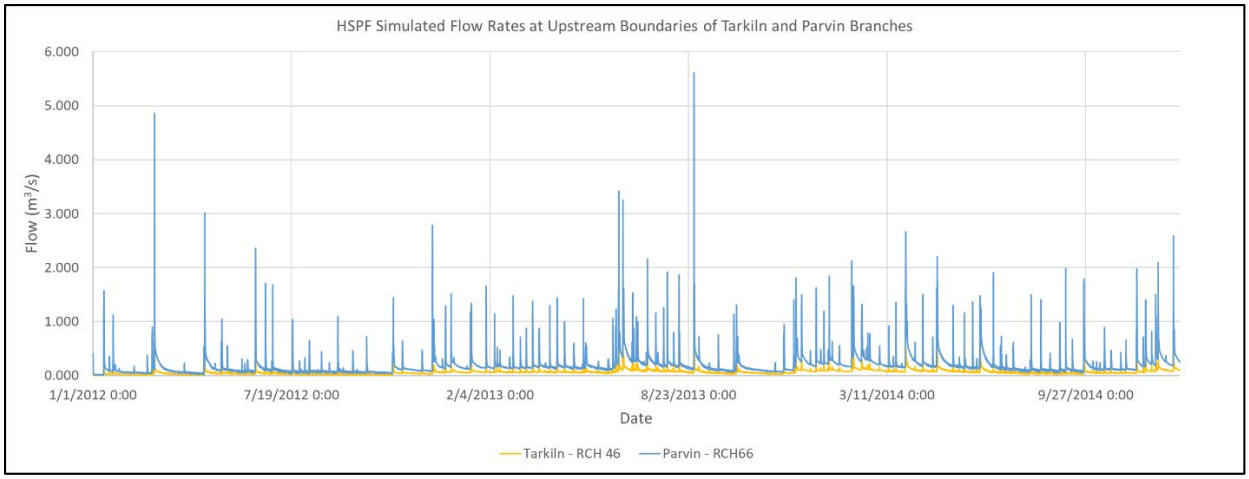

Figure 23: Simulated Flows at Tarkiln and Parvin Branches vs Measured Flow at Almond Road

CLEMSON UNIVERSITY HYDROGRAPH AND MODFLOW

CU Hydrograph was not calibrated because there were no parameters to update in the Excel worksheet. The historic precipitation data for Vineland, NJ, and the discharge data from the USGS gage 01411500 at Almond Road from 2007 to 2017 were used in the Excel program to calculate the baseflow flux based on the Wallingford Institute of Hydrology hydrograph separation analysis procedure (Wesselink & Gustard, 1992). Results from Chapter 3 show that the average groundwater discharge rate per segment of the Maurice River from 2012-2015 was 1.36 cfs [0.0385 cms].

ENVIRONMENTAL FLUID DYNAMICS CODE +

HYDRODYNAMIC MODEL

The hydrodynamic model was developed using the modified USGS gage measured discharge to represent the upstream boundary discharge for the Maurice River, the results from HSPF to represent the upstream discharge for each tributary including the surface runoff during precipitation events, and the results from CU Hydrograph to represent the groundwater discharge into the Maurice River. Calibration data for this hydrodynamic model were limited to the continuous discharge and gage height data from the USGS gage at Almond Road and the discharge measured on July 12, 2012 at Almond Road from the 3-year study (Figure 5). The model was supposed to be run from 2012-2015, but due to time constraints, the model was only run for six months. No additional data were available to validate the hydrodynamic model. Each time series of discharge for the Maurice River, BWB, Parvin Branch, and Tarkiln Branch were set up in the EFDC+ input file, QSER.inp, which assigns each upstream discharge time series to be used in the EFDC+ model domain. The simulated discharge and water surface elevation (WSE) from the six-month hydrodynamic model were compared to the available measured discharge and WSE data. Figure 24 shows the measured WSE from the USGS gage and the simulated WSE of the Maurice River at the Almond Road Weir over six months (February 2012 to August 2012). The relative bias at Almond Road (1.5%) was acceptable. The simulated WSE was higher than the measured WSE.

The measured gage height from USGS was used to calculate the measured WSE. As discussed in Chapter 3, the bottom elevations of the waterbodies were interpolated using elevation of each hydraulic structure and limited water depths measured in the field because the NJDEP elevation data did not include a bathymetric survey. Thus, the simulated WSE does not fully represent the measured WSE. A LIDAR bathymetric survey is expected to be completed in the Fall of 2024. With the uncertainty regarding the inaccurate bottom elevation data, and no additional measured WSE data, the agreement between the simulated WSE and measured WSE at Almond Road was considered adequate.

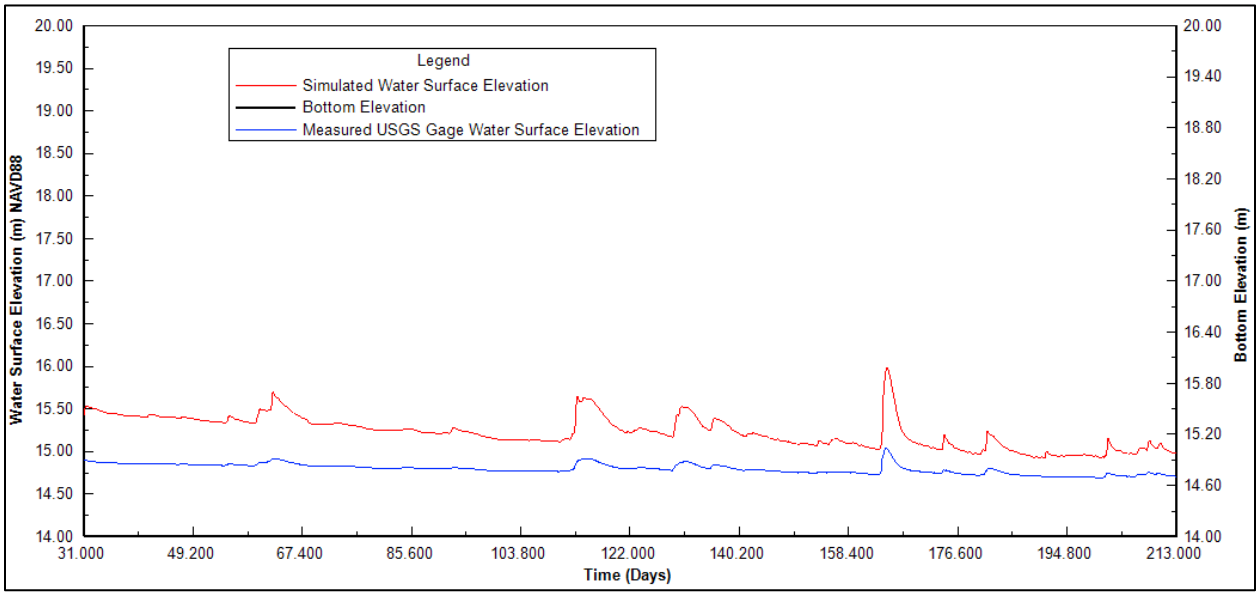

Figure 24: Measured WSE and Simulated WSE at Almond Road Weir

As discussed in Chapter 3, the measured discharge from the USGS gage at Almond Road was modified to represent the upstream discharge at Garden Road. Figure 25 shows that the simulated discharge at Garden Road is 4% less than the measured discharge at Almond Road to exclude the flow contribution from the BWB. The simulated discharge at Almond Road was compared to the measured discharge at Almond Road during the six-month run as shown in Figure 26. The simulated baseflow was representative of the measured baseflow, but the simulated storm flows were slightly overestimated compared to the measured storm flow. Because the upstream boundary for the Maurice River and BWB

were generated using modified measured data and semi-calibrated output from HSPF, it was anticipated that the simulated discharge at Almond Road would not be the same as the measured discharge at Almond Road. In a similar study, simulated discharges were evaluated using "specified model performance measures for both relative bias and median relative error of ± 10%" (Hayter et al., 2006). The relative bias for the discharge at Almond Road was -7.8% and this was acceptable. The simulated discharge at the upstream boundary of BWB for six months is shown in Figure 27. The measured discharge on July 12, 2012 (indicated by the blue marker) was used to compare the simulated discharge at BWB in EFDC+. The simulated discharge on July 12, 2012 (0.186 m^3/s) was within 1% of the measured discharge (0.187 m^3/s) with a relative bias of 0.5% and considered acceptable based on available data. The simulated discharges at the upstream boundaries for the Parvin and Tarkiln Branches are shown in Figure 28. The fluctuations indicated that there may have been instability in the model, but the small-scale fluctuations remained bounded. Despite the lack of measured discharge data, the HSPF simulated discharges for these tributaries were used for the EFDC+ boundary conditions since measured flows were not available.

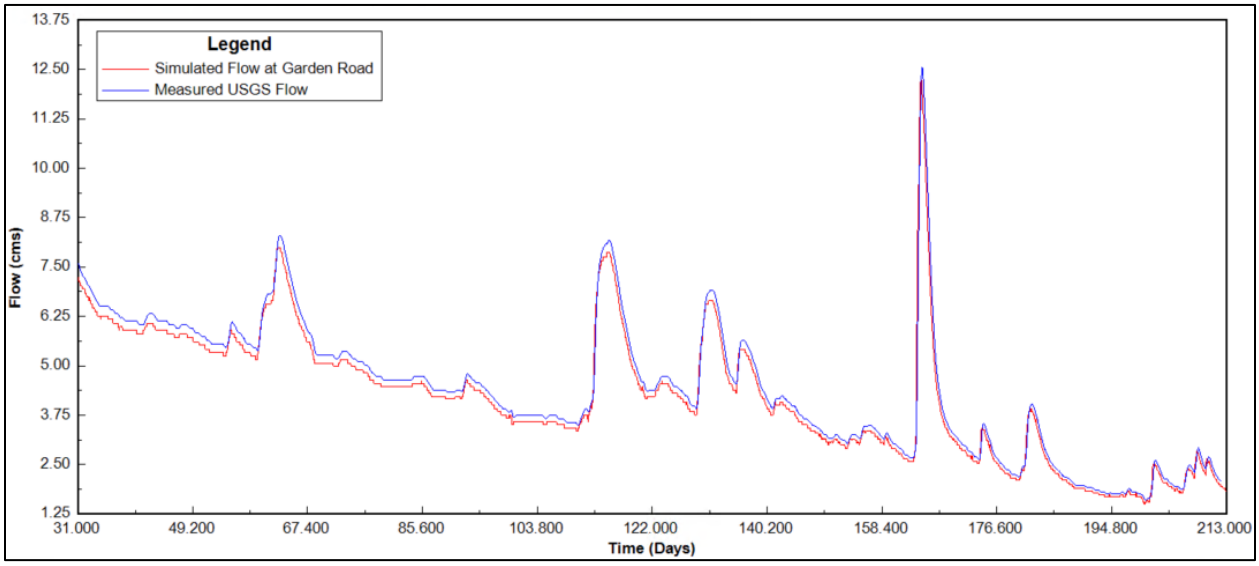

Figure 25: Measured Discharge from Almond Road and Simulated Discharge at Garden Road

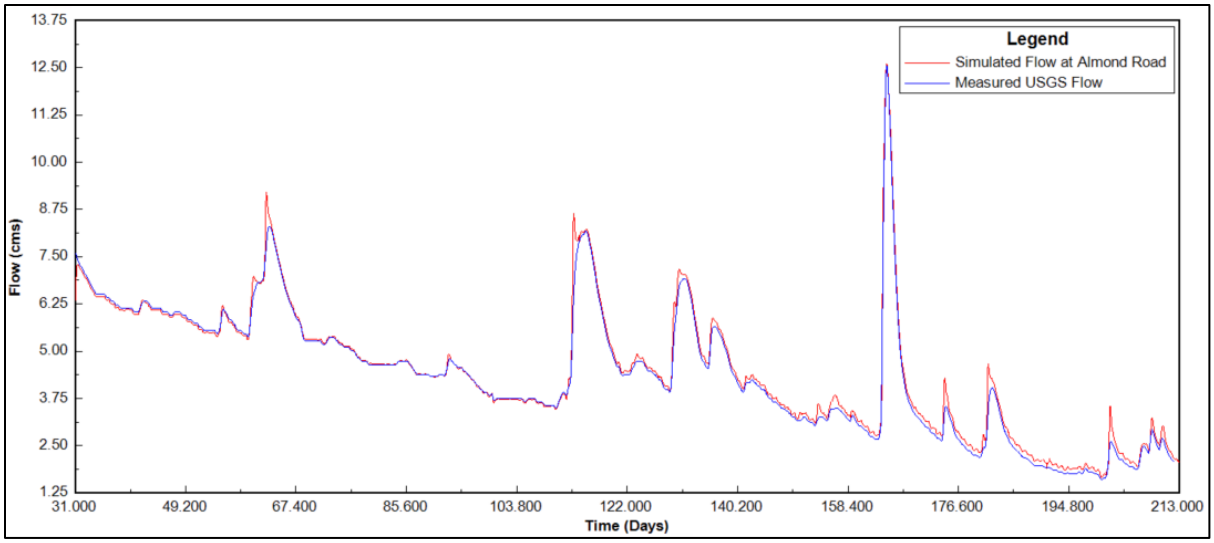

Figure 26: Measured Flow and Simulated Flow at Almond Road Weir

The simulated discharge of the Maurice River at Sherman Road (downstream of the confluence with the Parvin Branch) for six months is shown in Figure 29. The measured flow (indicated by the blue marker) for the Maurice River at Sherman Road on July 12, 2012, was 3.1 m^3/s and the simulated discharge was 2.5 m^3/s. The simulated discharge was within 20% of the measured discharge with a relative bias of -19%. This difference was mostly likely due to the reported limitations of the river bathymetry and the uncalibrated upstream discharges from the Parvin and Tarkiln Branches.

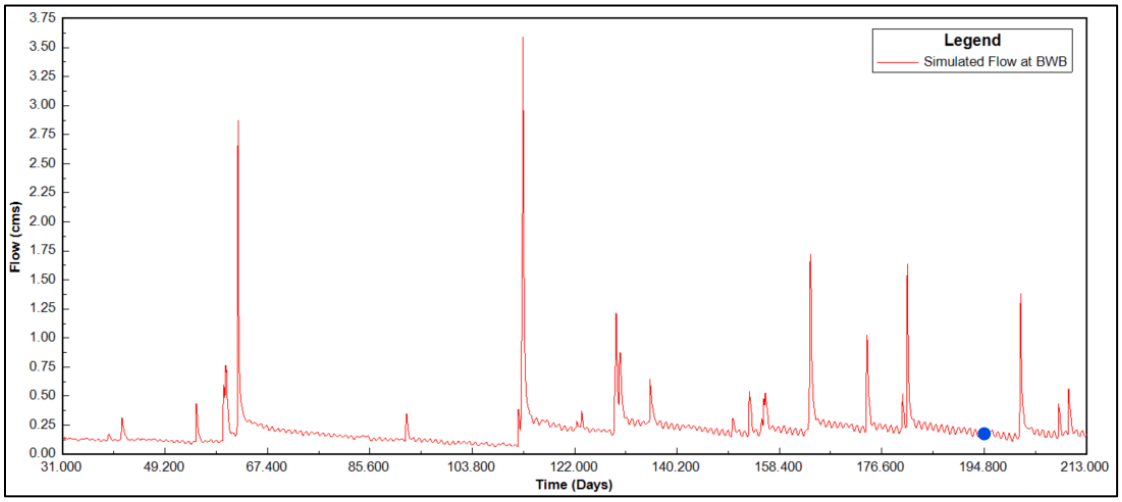

Figure 27: Simulated BWB Flow at Delsea Road (red) and Measured Flow (Blue Marker) on Day 194 (July 12, 2012)

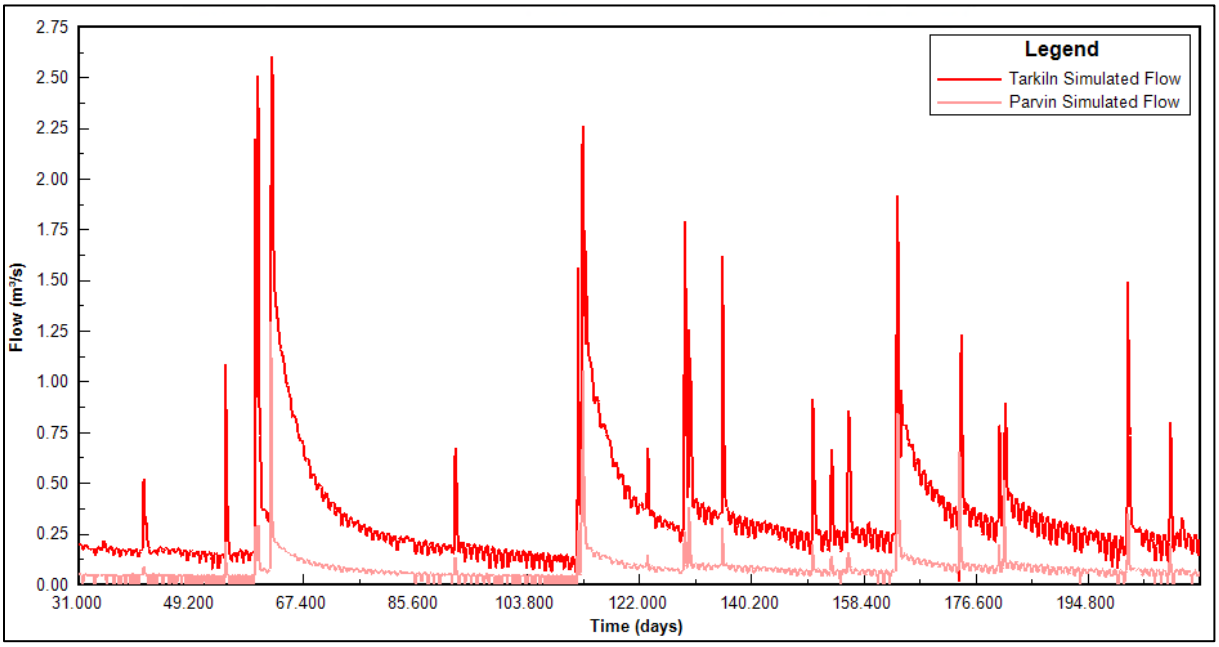

Figure 28: Simulated Flow in the Parvin (dark red) and Tarkiln (light red) Tributaries

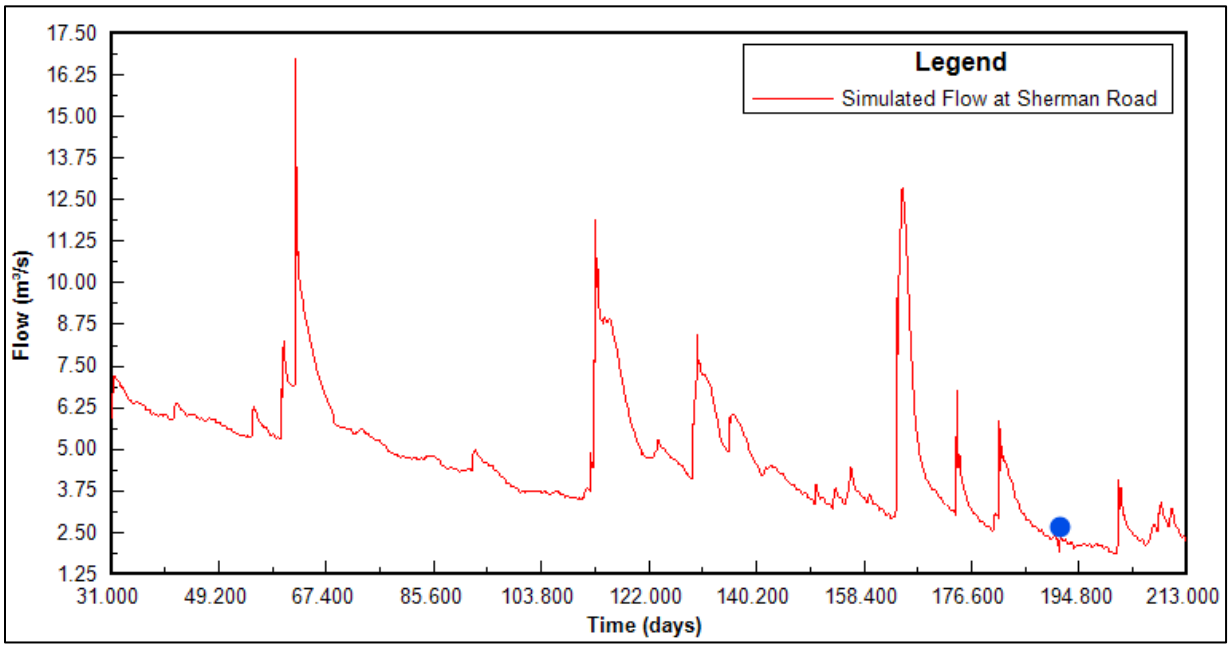

Figure 29: Simulated Flow in Maurice River at Sherman Road (red) and Measured Flow at Sherman Road on July 12, 2012 (blue circle)

SEDIMENT TRANSPORT MODEL

There were no data available to calibrate or validate the sediment transport model in EFDC+. Suspended sediment concentrations are scheduled to be measured in the summer of 2024 during high flow events to measure the quantity of sediment in suspension. The sediment transport model, SEDZLJ, was setup using the measured erosion rates, bulk densities, and grain size distributions from the SEDFLUME study completed in 2013 (Sea Engineering Inc., 2013). The suspended sediment concentration at the upstream boundaries of each tributary was set to zero. The suspended sediment concentration at the upstream boundary of the Maurice River at Garden Road was calculated using a regression analysis based on the Maurice River discharge. Though not calibrated or validated, the use of measured site-specific sediment bed parameters was thought to lend credibility to using this sediment transport model in EFDC+.

For example, the sediment transport model demonstrated that it was capable of simulating erosion and deposition. For example, upstream of the Almond Road weir in the backwater area caused by the weir, the shallow side banks of the Maurice River had reduced flows which allowed for suspended sediments to deposit thereby increasing the bed thickness. Directly downstream of the weir, as the water passed over the weir, the higher flows and therefore the higher bed shear stresses caused the sediment bed to erode. Figure 30 shows the deposition and erosion upstream and downstream of the weir at the conclusion of a short one-month simulation. Quantitatively, these results are consistent with expected erosion and deposition patterns for a river with a hydraulic structure in place. The increase in bed thickness is very small; however, this is attributed to the short simulation period of one month with no significant high flow events.

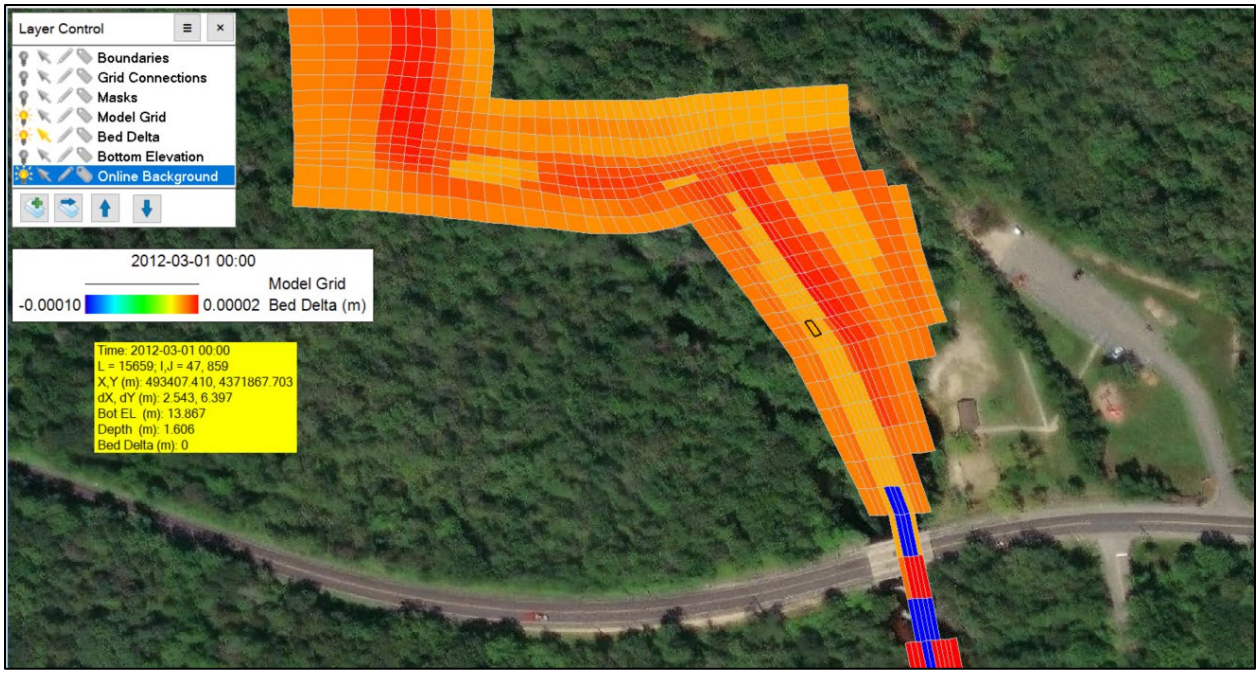

Figure 30: Bed Delta Upstream and Downstream of Almond Road Weir Indicating Deposition and Erosion Patterns

CONTAMINANT TRANSPORT MODEL

The contaminant transport model was partially calibrated using data from the 3-year study (Lockheed Martin SERAS, 2015). The measured data collected on July 14, 2012 included total and dissolved arsenic concentrations from the sediment and surface water samples collected at Alliance Beach, Almond Road Beach, and BA Beach as shown in Figure 6. Due to the high density of samples collected at each location, an average arsenic concentration in the sediment bed was used to represent each location. After running the contaminant transport model for 2.5 weeks (July 2012), there were no drastic changes in the sediment bed concentrations at these locations due to the short simulation period. Table 6 shows the average measured concentration compared to the average simulated arsenic concentration in the sediment bed.

To test the contaminant transport model and check if the model's calculated contaminant concentrations behave as anticipated, a sensitivity test was completed by varying the DIFTOXS parameter (diffusion flux coefficient) in EFDC+. This parameter controls the flux of a contaminant

moving from the top layer of the sediment bed to the water column. A higher DIFTOXS value should increase the concentration of arsenic in the water column and decrease the sediment bed arsenic concentration while a low DIFTOXS value should only slightly decrease or maintain sediment bed arsenic concentrations because less arsenic is diffused into the water column. This testing has been completed in previous studies to check a model's ability to represent contaminant transport (Hayter et al. 2014).

The results from this sensitivity test (Table 6) show that the model quantitatively behaves as expected. The sensitivity test was applied at sample locations from Alliance Beach, Almond Road, and BA Beach. Each measured arsenic concentration in the sediment bed is shown in bold font. The next three columns show the arsenic concentration in the sediment bed from the original simulation, the high DIFTOXS simulation, and the low DIFTOXS simulation, respectively. The original DIFTOXS value was set to 1E-10 m^2/s. When the DIFTOXS parameter was increased to 1E-8 m^2/s the sediment bed concentration decreased by 0.4 mg/kg. When the DIFTOXS parameter was decreased to 1E-12 m^2/s the sediment bed concentration did not change, or slightly decreased. While this testing was only completed for a 2.5-week simulation period, the results indicated the model is quantitatively behaving as expected based on the average values.

Table 6: Sensitivity Testing on Sediment Bed Arsenic Concentration

SEDIMENT BED ARSENIC CONCENTRATION SENSITIVITY TESTING					
Sampling Location		**Actual Bed (mg/kg)**	Simulated Sediment Bed Concentration (mg/kg) DIFTOXS = 1E-10 m^2/s	Simulated Sediment Bed Concentration (mg/kg) DIFTOXS = 1E-8 m^2/s	Simulated Sediment Bed Concentration (mg/kg) DIFTOXS = 1E-12 m^2/s
Alliance	A1-9W.30	**0.70**	24.59	24.32	24.58
	A1-11E.10	**0.60**	24.60	24.35	24.60
	A1-10E.0	**0.50**	24.60	24.35	24.60
	A1-6.30	**56.00**	24.62	24.33	24.60
	A1-6.50	**43.00**	24.62	24.33	24.60
	A1-2.20	**11.00**	24.61	24.33	24.61
	A1-6.40	**1.70**	24.62	24.34	24.60
	A1-4.70	**0.60**	24.61	24.36	24.60
	A1-7E.-5	**129.00**	24.62	24.35	24.10
	A1-7W.0	**2.60**	23.98	23.07	23.98
	A1-7W.-5	**60.00**	23.97	23.06	23.94
	A1-2.90	**2.80**	24.60	24.36	24.58
	A1-3.30	**64.00**	24.61	24.33	24.60
	A1-1.50	**0.50**	24.55	24.34	24.53
	A1-1.75	**2.50**	24.54	24.35	24.52
	AVERAGE	**25.03**	24.52	24.17	24.47
Almond					
	A2-17	**57.00**	18.62	18.54	18.62
	A2-12	**1.30**	18.67	18.56	18.65
	A2-22	**1.50**	18.93	17.49	18.90
	A2-27	**78.00**	18.91	18.93	18.90
	A2-43	**1.00**	18.83	18.83	18.84
	A2-32	**2.60**	18.80	18.80	18.81
	A2-37	**1.50**	19.01	19.01	19.01
	A2-48	**6.30**	18.63	18.55	18.60
	A2-53	**60.00**	17.80	17.45	17.76
	A2-57	**1.20**	18.63	18.56	18.60
	A2-62	**43.00**	18.65	18.57	18.62
	A2-67	**0.60**	17.77	17.62	17.75
	A2-72	**1.40**	18.62	18.55	18.60
	A2-77	**16.00**	18.53	18.54	18.50
	AVERAGE	**19.39**	18.60	18.43	18.60
BA Beach					
	A4-16	**0.90**	4.54	4.50	4.54
	A4-12	**0.80**	4.53	4.49	4.53
	A4-06	**15.00**	4.47	4.46	4.47
	A4-01	**1.30**	4.49	4.46	4.50
	AVERAGE	**4.50**	4.51	4.48	4.51

Figure 31: Area (Circled in Red) Downstream of Almond Road Weir Shows Increased Bed Shear Stress During High Flow Event in June 2012

To further demonstrate the model's ability to simulate sediment and contaminant transport, the model was used to simulate a high flow event that occurred on June 13, 2012. During a high flow event, the bed shear stresses increase and potentially exceed the critical shear stress of erosion of the sediment bed. The model was run for June 2012 to check if it did simulate sediment erosion that resulted in a decrease in sediment bed thickness and an increase in the water column arsenic concentration caused by resuspension of contaminated sediment and porewater release. Figure 31 shows the red circle indicating the location of the grid cell selected to demonstrate the simulated results. This grid cell was selected because it was in the main channel of the Maurice River downstream of Almond Road and experienced a higher increase in bed shear stress compared to other surrounding cells. As the simulation approached the high flow event on June 13th (164th day of the year), the bed shear stress increased (Figure 32). The high flow caused the bed shear to increase and once this shear exceeded the critical shear stress (0.3 Pa), the sediment bed eroded and caused an increase in the suspended sediment concentration as shown in Figure 33. Figure 34 shows the arsenic concentration in the top layer of the sediment bed and the bed delta. During the storm on day 164, the bed delta decreased indicating the bed layer thickness has decreased due to erosion. The initial arsenic concentration (19 mg/kg) spiked up to 70 mg/kg and then decreased during the high flow event as contaminated sediments eroded from the bed and contaminated porewater released into the water

column. The arsenic spike is a numerical artifact resulting from the discretized sediment bed layers. Each of the 7 layers has the same constant concentration of arsenic. Originally, layer 3 was the top layer of the bed, but once deposition occurred the less contaminated sediment deposited on layer 2 which becomes the new top layer with a reduced arsenic concentration. During the high flow event, sediment from layer 2 is eroded and layer 3 became the top layer with the original arsenic concentration, but as sediment redeposited, layer 2 was reactivated and the arsenic concentration in the sediment bed layer decreased. The quick exchange between layer 2 and 3 and the varying arsenic concentration in the top bed layer caused the EFDC+ routine to malfunction. Even with this numerical artifact, the model recovered quickly, and the arsenic concentration decreased. This short model demonstration showed that the arsenic concentration in the sediment bed did not significantly change, but the high flow events did cause erosion of the bed including a small increase of arsenic in the water column as shown in Figure 35. The average concentration of arsenic in the water column was less than 0.1 μg/L. The arsenic in the water column was mostly bound to DOC (72%) or dissolved (28%). During the high flow event, arsenic bound to sediment increased the arsenic concentration in the water column, however, less than 1% of the arsenic in the water column was bound to POC. Without having a measured arsenic partition coefficient for organic matter, the partition coefficient was overestimated using the arsenic partition coefficient from literature (Allison & Allison, 2005). The arsenic partition coefficient for organic matter should be measured or estimated using a model like PHREEQC to simulate and better represent the concentration of the three phases of arsenic in the water column. These demonstrations showed that even during a short simulation period, the hydrodynamic, sediment transport, and contaminant transport models responded to parameter adjustments controlling the transport of arsenic or high flow events. Due to the short simulation runs and the limited measured data available for calibration, the three-tier modeling system could not be fully calibrated and validated, but the model could still be used to simulate two potential remediation scenarios as discussed in the next chapter.

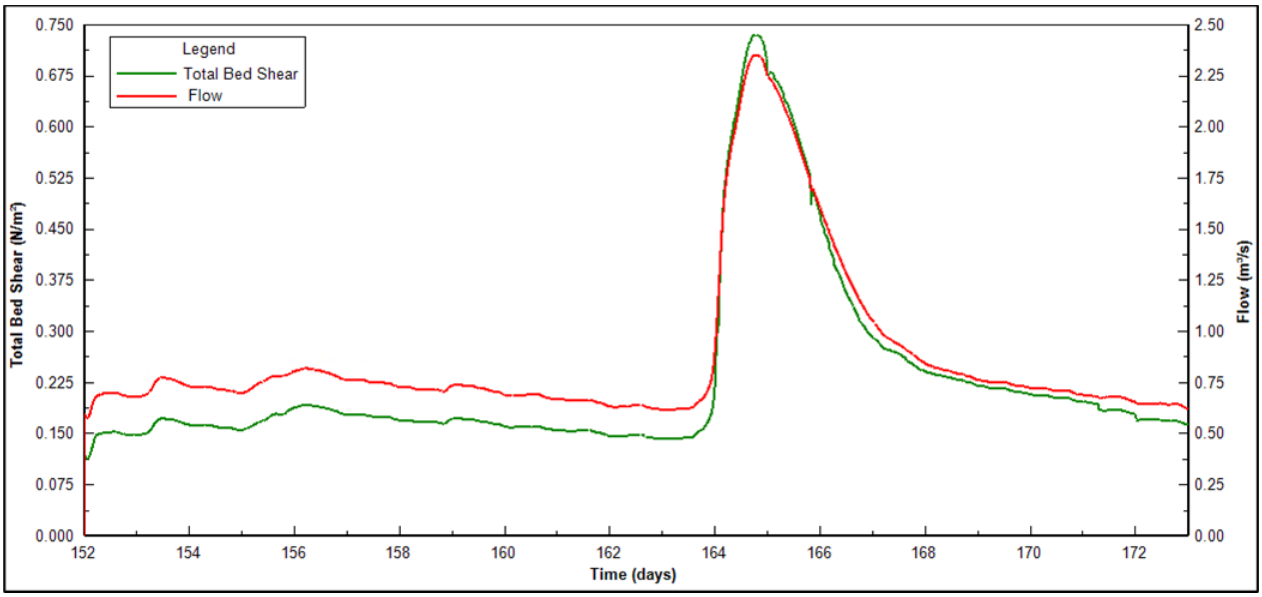

Figure 32: Simulated Flow vs. Bed Shear Stress Downstream of Almond Road

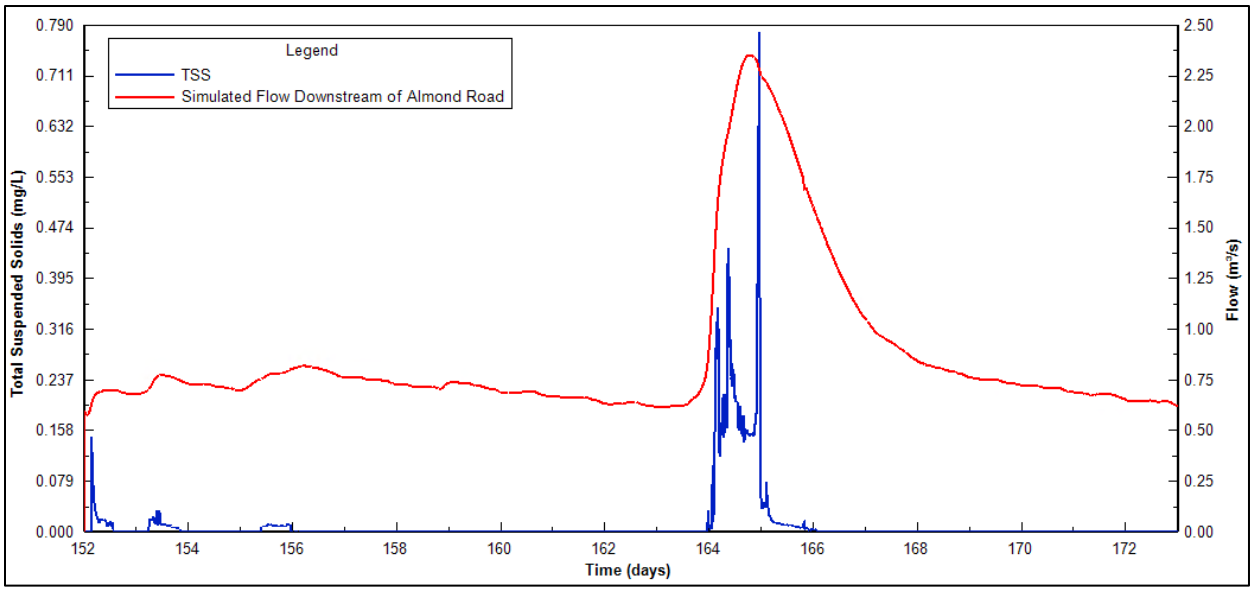

Figure 33: Simulated Flow vs. Total Suspended Solids Downstream of Almond Road

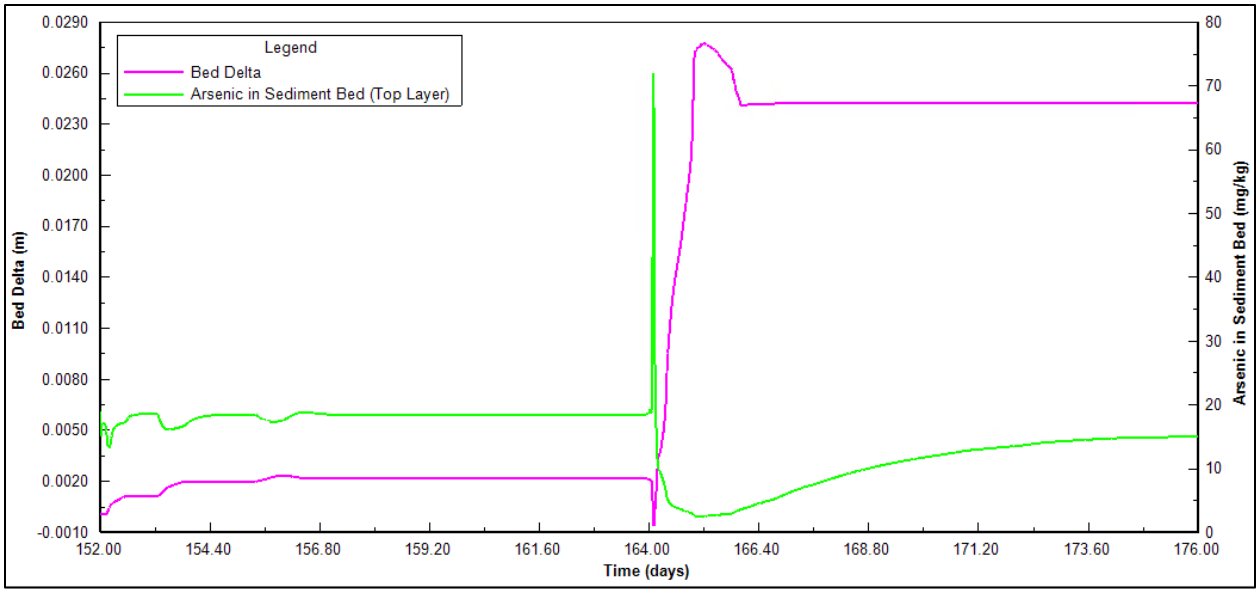

Figure 34: Change in Arsenic Concentration in Top Layer of Sediment Bed Downstream of Almond Road During High Flow Event

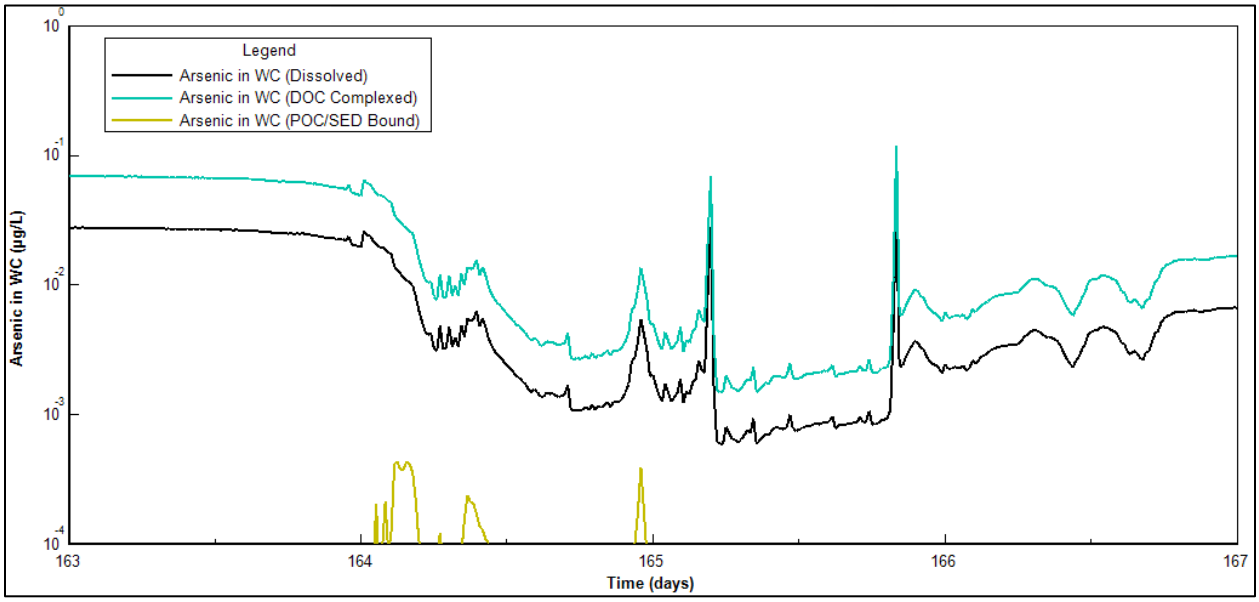

Figure 35: Three Phases of Arsenic in WC During High Flow Event Downstream of Almond Road

V. MODEL SIMULATION/APPLICATION

The calibrated EFDC+ model was used for a short-term demonstration to simulate two potential remediation alternatives for the Vineland Chemical Superfund site to compare and evaluate both remediation options.

1.) Post-Remediation of Blackwater Branch – Monitor Natural Attenuation: This passive remediation plan monitors the contaminated site without any remediation action. Over time, during high flow events, the contaminated sediments naturally erode and clean, upstream sediments deposit on the sediment bed. To represent the remediated BWB, the initial total arsenic concentration in the BWB and its floodplains was changed to 0 mg/kg and 0 μg/L to represent a fully decontaminated site in both the sediment and surface water. This simulation ran for six months, and the results are discussed in the next section.

2.) Remediation of Blackwater Branch and Maurice River Upstream of Almond Road: This remediation plan includes bank-to-bank dredging the sediment in the Maurice River from the confluence with BWB down to Almond Road. The sampling from the three-year study indicated that there were hot spots of arsenic in this reach of the Maurice River. To represent the dredged portion of the Maurice River, the initial total arsenic concentration for this reach was set to 0 mg/kg and 0 μg/L. The simulation ran for six months, and the results are discussed in the next section.

RESULTS

The following section describes the results from the three-tier contaminant fate and transport modeling system after simulating the two selected remediation alternatives for six months (February 2012 to August 2012). Typically, remediation alternatives are run for multiple years to assess the long-term impact, but for this research, the 6-month run was considered appropriate to partially evaluate the effectiveness of each remediation plan and observe similarities and differences between each alternative.

For Alternative 1, arsenic transport results from Alliance Beach, Almond Road, downstream of Almond Road, and BA Beach were evaluated (Figure 6). The arsenic concentration in the sediment bed of the Maurice River at Alliance Beach decreased by 1.2% during the six-month simulation. Figure 36 shows the arsenic concentration decreased over time as the bed delta increased. The bed delta increased after high flows decreased indicating that sediment deposited onto the bed. The green line represents arsenic concentration in the top layer of the bed. The arsenic concentration in the top layer decreased to 0.5 mg/kg indicating that some of the upstream sediments deposited and formed a thin top layer of less contaminated sediments. Additionally, the arsenic concentration decreased as the contaminant diffused into the water column. Overall, the arsenic concentration in the sediment bed of the Maurice River at Alliance Beach (approximately 400m [0.25 miles] from the remediated tributary) did not significantly decrease indicating that the remediation of BWB did not have significant impacts on the transport of arsenic downstream in the Maurice River over the six-month period. For Alternative 2, Alliance Beach was included in the remediated area and there were no results to evaluate from this model.

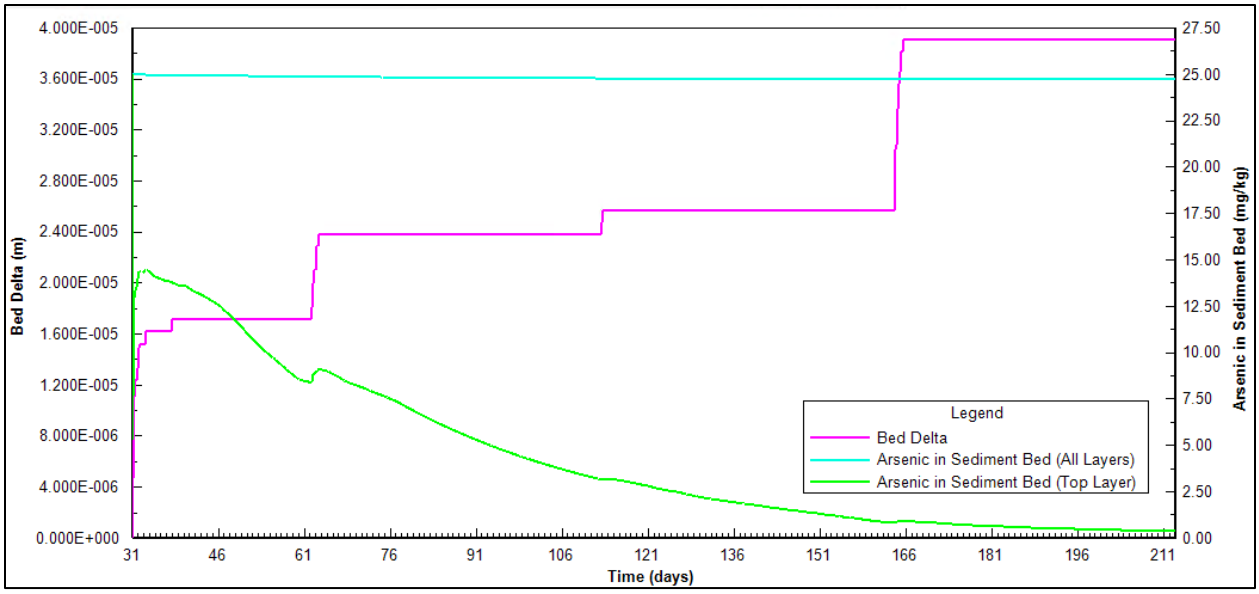

Figure 36: Arsenic Concentration in Sediment Bed versus Bed Delta at Alliance Beach

For Alternative 1, the arsenic concentration in the top layer of the sediment bed of the Maurice River at Almond Road also decreased during the six-month simulation as shown in Figure 37. During the first month, the arsenic concentration in the top layer decreased to 1.1 mg/kg as arsenic diffused into the water column. After the first high flow event on day 62, the bed delta increased (micro-scale), and the arsenic concentration decreased as a new less contaminated top layer formed from the depositing sediment. During the next two high flow events on days 113 and 164, the top layer concentration remains unchanged indicating that these high flow events did not disrupt the new, less contaminated top layer. Overall, the arsenic concentration in the sediment bed of the Maurice River at Almond Road did not significantly change (decreased by 1.1%) which is consistent with the results from Alliance Beach. The Maurice River at Almond Road is approximately one mile from the confluence with the BWB. Over the short simulation period, Alternative 1 did not appear to have a significant role in the transport

of arsenic from the sediment bed of the Maurice River at Almond Road. For Alternative 2, Almond Road was included in the remediated area and there were no results to evaluate from this model.

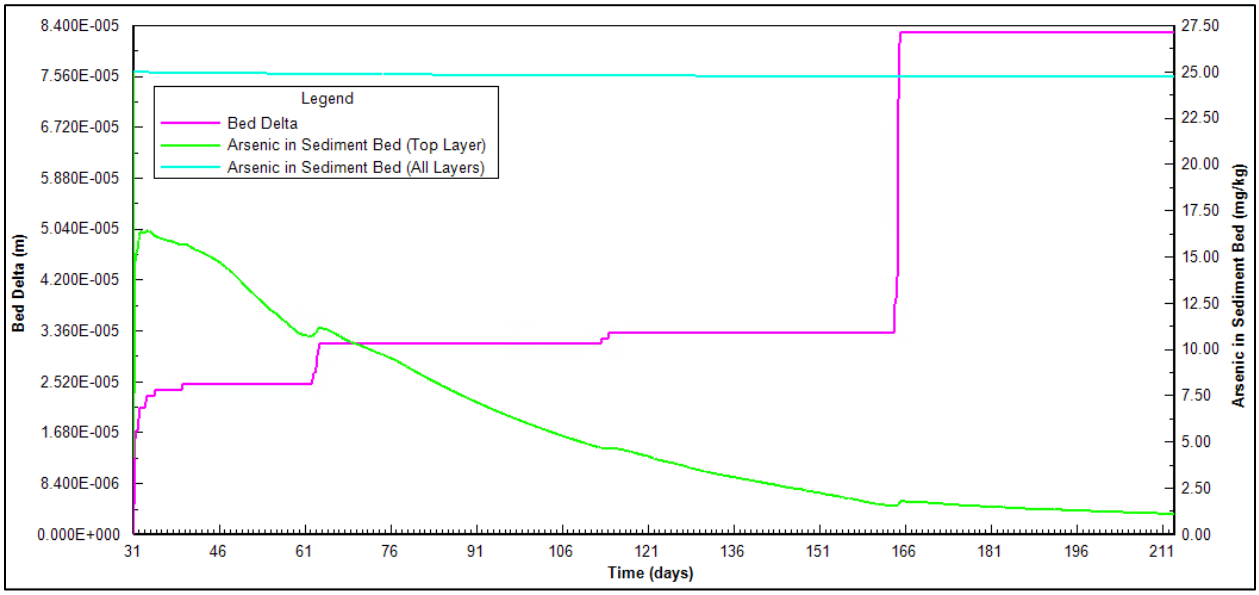

Figure 37: Arsenic Concentration in Sediment Bed versus Bed Delta at Almond Road

The results from Alternative 1 and Alternative 2 were compared at two locations: downstream of Almond Road and BA Beach. These locations were selected because sediment and surface water samples were collected and analyzed for arsenic at each location during the three-year study. The arsenic in the sediment bed from Alternative 1 was the exact same for Alternative 2 at each of these locations in the model domain. This indicated that the model run time was not long enough to differentiate between the two remediation alternatives and that during the 6-month period, the sediment bed concentration was not affected by the removal of contaminated sediments from the BWB confluence down to Almond Road.

The arsenic concentration in the sediment bed of the Maurice River downstream of Almond Road (approximately 400m [0.25 miles]) did not change between Alternative 1 and 2 so results from Alternative 1 and 2 are shown in Figure 38. Similar to the results from upstream (Alliance Beach and Almond Road), the arsenic concentration in the top layer of the sediment bed decreased. During the

high flow events on day 62, 113, and 164 the arsenic concentration spiked up and then instantly decreased. The extreme increase in arsenic concentration at the beginning of each high flow event also occurred during the partial calibration of the contaminant transport model at the same location. This numerical artifact appeared again due to the discretization of the sediment bed layers as described in Chapter 4, but it also recovered instantly. Despite this numerical error, the results were still consistent with the upstream locations. The TSS increased during the high flow events as upstream suspended sediments were transported downstream into this grid cell and as sediment eroded from the bed. In this grid cell, the bed delta was a very small negative value indicating that there was some erosion of sediment from the bed particularly during the high flow events. The arsenic concentration in the top layer decreased as sediments eroded into the water column and porewater was released from the bed into the water column. Outside of the high flow events, the steady decline in the arsenic concentration was due to arsenic diffusing into the water column from the top layer. However, the overall arsenic concentration in the sediment bed only reduced by 0.2%.

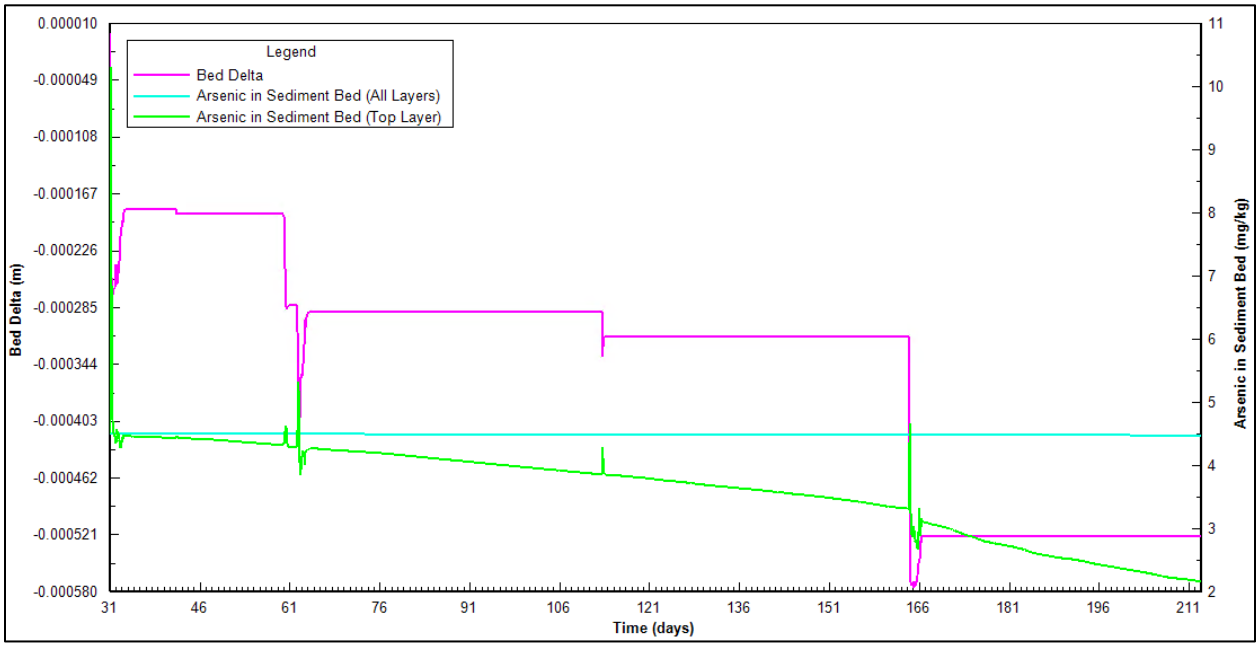

Figure 38: Arsenic Concentration in the Sediment Bed versus Bed Delta Downstream of Almond Road

At this grid cell downstream of Almond Road, the change in arsenic concentration in the water column was insignificant between both alternatives. During the short simulation period, the average arsenic concentration in the water column at this grid cell for Alternative 1 was 0.005 μg/L. The average arsenic concentration in the water column at this grid cell for Alternative 2 was 0.004 μg/L. During the largest high flow event, the maximum arsenic concentrations in the water column for Alternative 1 and 2 were 0.024 μg/L and 0.023 μg/L, respectively. Alternative 2 had slightly lower concentrations in the water column because a greater upstream portion of the Maurice River was remediated and therefore there was less available arsenic in the water column. In both alternatives, the increase in arsenic concentration during the high flow events was a result of upstream arsenic transported downstream and arsenic from the sediment bed diffusing into the water column, but overall, the concentration of arsenic in the water column decreased from the initial concentration (1.3 μg/L) as advective flow transported the contaminant downstream. In both alternatives, the concentration of arsenic bound to POC was very low throughout the entire six months indicating that most arsenic bound to solids remained in the bed while freely dissolved arsenic and colloidal-bound arsenic were found in the water column during the high flow events. Overall, the concentration of arsenic in the sediment bed and water column of the Maurice River downstream of Almond Road did not significantly change, implying that neither alternative had significant impacts on the downstream transport of arsenic during this short simulation period.

The arsenic concentrations in the sediment bed of the Maurice River at BA Beach for both alternatives are shown in Figure 39. During the high flow events on days 62, 113, and 164, the bed delta values are negative indicating that sediment eroded due to the high shear stress exceeding the critical shear stress (0.3 Pa). After the flows reduced, the sediment bed thickness increased as indicated by the positive bed delta value. The top layer of the sediment bed decreased as arsenic diffused from the bed to the water column, but during each high flow event, the concentration briefly increased until the flow

event ended, and the sediment bed thickness increased. During each high flow event, less contaminated sediments eroded from the sediment bed and suspended into the water column as shown in Figure 40. This was confirmed by comparing the TSS concentration of the surrounding grid cells and verifying that the increase in TSS was in part due to a contribution of sediments from the bed. After the flow event, the sediment from upstream began to deposit, and a thin, less contaminated bed layer was formed. Overall, the sediment bed concentration only reduced by 0.6% during the six-month simulation concluding that both alternatives did not significantly impact the transport of arsenic downstream at BA Beach. This was anticipated after evaluating the results from Alliance Beach, Almond Road, and downstream of Almond Road.

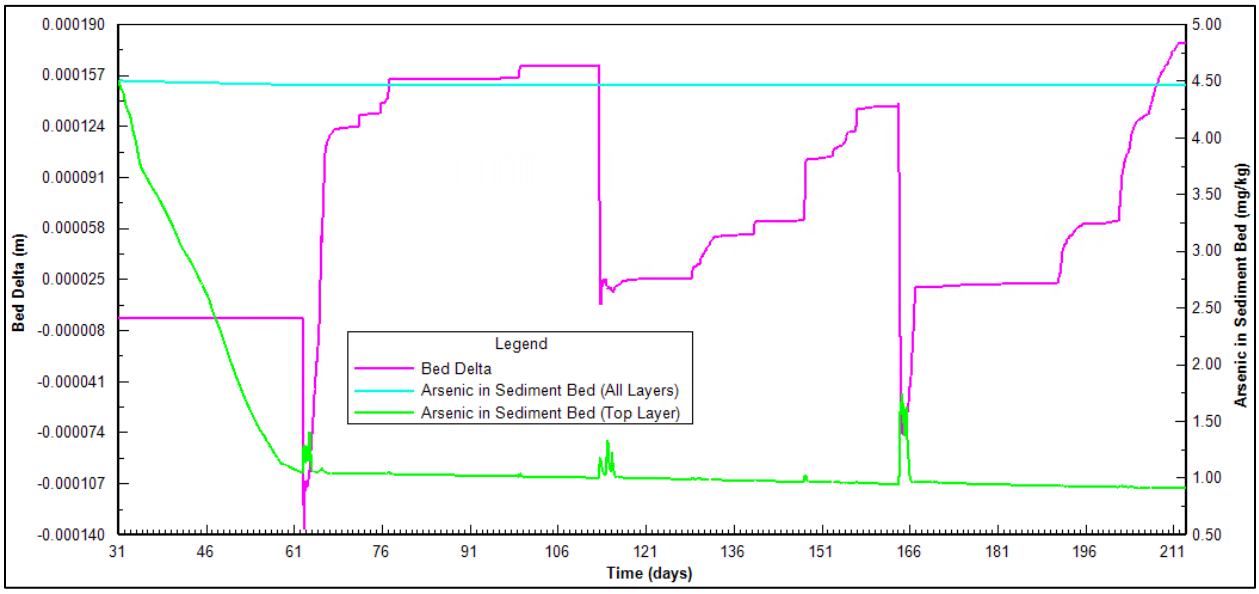

Figure 39: Arsenic Concentration in Sediment Bed versus Bed Delta At BA Beach

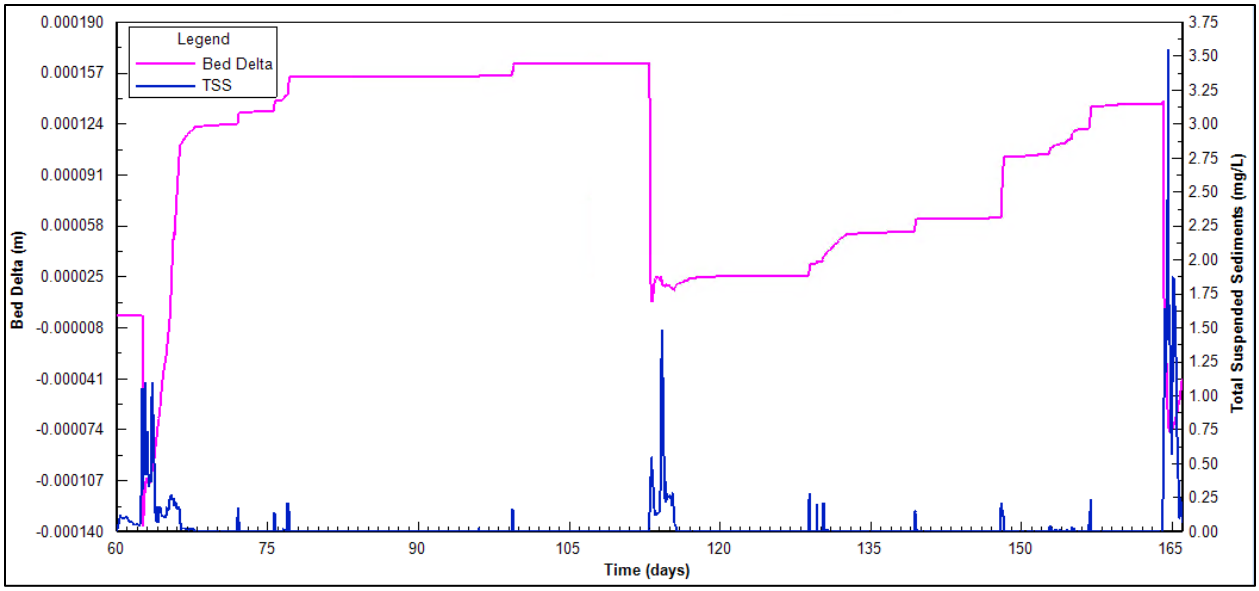

Figure 40: TSS Concentration during High Flow Events versus Bed Delta at BA Beach

The groundwater discharge input into EFDC+ did not affect Alternative 1 nor 2. Both simulations were run with and without the groundwater discharge added to the hydrodynamic model, and no noticeable change occurred because the average groundwater discharge into each grid cell representing the Maurice River was extremely small, 5E-5 m^3/s. If the groundwater discharge was higher, the groundwater could affect the sediment bed concentration of arsenic in both alternatives by increasing or decreasing the arsenic concentration in the sediment bed. As groundwater flows into the pore spaces of the subsurface sediments, porewater pressure increases and forces contaminated porewater to release into the water column. Groundwater, if contaminated, could re-contaminate the sediment bed which has been an ongoing issue at the Vineland Chemical Superfund site. In contrast, clean groundwater could transport dissolved arsenic into the river. These groundwater interactions were not represented in these simulations due to the limitation of the three-tier model described above.

VI. SUMMARY AND CONCLUSIONS

The following summary and conclusions for this modeling study are discussed below. The three-tier modeling system was developed and run to simulate the transport of total arsenic through a portion of the Maurice River watershed. Even with uncertainty in the output from HSPF and CU Hydrograph, the hydrodynamic model simulated flows in the Maurice River, Blackwater Branch, Tarkiln, and Parvin Branch that were comparable to the available measured discharge data. The hydrodynamic model produced simulated flows within the Maurice River with an average percent difference of 8% from that measured at the USGS gage 01411500 at Almond Road in Norma, NJ.

The groundwater discharge from CU Hydrograph was important to include in this modeling study to represent the Maurice River, a gaining reach. However, it was not the driving force for the hydrodynamic model nor was it influential on the results of Alternative 1 and 2. The average groundwater discharge rate was 0.8% of the average Maurice River flow.

The sediment transport model was not calibrated; however, it was developed using measured sediment properties from the SEDFLUME study performed at the site in 2013. Quantitatively, the model behaved as expected, simulating deposition in the backwaters of the Maurice River created by the spillway across the river (a component of the USGS gaging station) where flow velocities were reduced in the area upstream of the weir, and erosion downstream of the weir as water flowed across the weir at higher velocities.

The contaminant transport model simulated the transport of arsenic in the dissolved, colloidal-bound, and particulate-bound phases. Sensitivity testing confirmed that the transport of arsenic from the bed to the water column via diffusion was represented by adjusting the diffusion flux coefficient, DIFTOXS. The model also demonstrated that it could simulate transport of arsenic during high flow events. As the flow rate increased, the bed shear stress increased and exceeded the critical shear stress

for erosion causing erosion of the finer sediments from the top layer of the sediment bed. The suspended sediments included contaminated and less contaminated sediments from upstream reaches of the Maurice River and thus, there was an increase in arsenic concentration in the water column dominantly in its dissolved and DOC-bound phases due to the high arsenic partition coefficient for organic carbon. The dissolved arsenic concentration increased due to porewater released into the water column and arsenic desorbing from sediment. There was minimal POC-bound arsenic in the water column indicating that most arsenic remained bound in the sediment bed. The arsenic partition coefficient for organic carbon was overestimated resulting in the unusually high and low concentrations of DOC-bound arsenic and POC-bound arsenic in the sediment bed, respectively.

The short-term demonstration of the three-tier model simulated and compared two remediation alternatives and showed that overall, the transport of arsenic during the six-month simulation was minimal – the average arsenic concentration in the sediment bed decreased by 1% across the model domain. During high flow events, the increased storm flow increased the bed shear stress and the model responded by simulating erosion of sediments from the top layer of the bed into the water column. Once flow returned to base levels, the bed delta began to increase (micro-scale), and sediments deposited onto the bed. Despite the short modeling period, the model results indicated that the arsenic concentration in the sediment bed began to decrease as arsenic diffused into the water column and less contaminated sediments deposited onto the bed. Overall, the 6-month modeling period was not sufficient to compare long-term impacts of Alternative 1 and 2, therefore, there was no detectable difference between the arsenic concentrations in the sediment bed downstream of each remediated area. The shorter modeling period did not allow enough time for upstream sediments to be transported downstream. The results from Alternative 1 and 2 can be used for a preliminary analysis of alternatives but should not be further evaluated until the model has run for a longer period.

The PHREEQC model calculated the fraction of As(3) and As(5) present at the 16 groundwater wells near the Vineland Chemical Superfund site. The results from PHREEQC showed that the arsenic was present in its less toxic form, As(5), at each of the 16 wells. These results cannot be applied sitewide because the groundwater and aquifer environment are not isotropic nor homogenous and the model is dependent on site-specific data to effectively represent the distribution of arsenic species. Overall, this modeling tool demonstrated that the arsenic is stabilized in the subsurface sediments and unlikely to pose an immediate risk to humans.

This research showed that individually, the three-tier contaminant fate and transport modeling system and PHREEQC provide useful information for decision makers and risk assessments. The current capabilities of each model are sufficient to support most remediation projects that are interested in evaluating and comparing remediation alternatives or assessing and quantifying the risk associated with a particular contaminant at a Superfund site. This thesis demonstrated that each of these models could be used to improve our understanding of how arsenic behaves at the Vineland Chemical Superfund site and predict the effectiveness of two potential remediation alternatives. Moreover, future research may consider potential opportunities to use these models together. Current, contaminant transport models like EFDC+ simulate the transport of total arsenic. However, there may be a need to simulate the transport of arsenic species or use the predicted arsenic concentrations from EFDC+ and use these data in PHREEQC to predict the arsenic species in a localized area with high arsenic concentrations. Further research and investigation would need to be conducted to determine if such a capability would benefit future contaminant transport modeling studies.

VII. RECOMMENDATION

The following section describes recommendations to build upon and improve the current research. It is important to recognize that the models used in this research are just tools, and they cannot provide all the answers. However, if a modeling study includes sediment and contaminant transport modeling, consider using EFDC+ or a three-tier modeling system, if applicable, to provide modeling results that can be used to support decision makers and provide insight into the effectiveness of potential remediation plans.

Due to the limited measured data available, the three-tier modeling system could not be fully calibrated and validated. Once the following data gaps are addressed, the three-tier modeling study can be fully calibrated and validated to provide results with less uncertainty. Data gaps include:

- Complete a bathymetric survey to update the bottom elevation of the water bodies used in the EFDC+ model domain to improve representation of the Maurice River, BWB, Parvin and Tarkiln Branches, and Union Lake and improve the calibration of EFDC+.
- Measure suspended sediment concentrations during and after high flow events to use in calibrating the SEDZLJ sediment transport model.
- Measure discharge of Maurice River at Garden Road and tributaries for one continuous year to update the calibration of HSPF and hydrodynamic models.
- Re-evaluate MODFLOW output and determine the appropriate groundwater discharge time series (2012-2015) to improve representation of the groundwater discharge into the Maurice River.
- Measure the organic carbon-water partition coefficient for arsenic to improve representation of arsenic concentrations in the water column.

To calibrate and validate the EFDC+ model, the model should be run for three years (2012-2015) to represent the full duration of the three-year flushing study. Afterwards, the two remedial alternatives should be run for at least five years. The longer simulation period would allow all measured discharge data from the three-year flushing study to be used in the calibration and validation of EFDC+. Running the remedial alternative simulations for five years or more, would allow for the hydrodynamics and sediment and contaminant transport processes to change the sediment bed and arsenic concentrations across the model domain and allow for further evaluation and comparison of the remediation alternatives with the goal of determining which alternative is more effective.

The PHREEQC model demonstrated how it can be used as a tool calculate the arsenic speciation in groundwater with site-specific data, but collecting more mineralogy data will improve model results. The aquifer should be analyzed to determine all dominant minerals present in the groundwater environment that arsenic may sorb to.

REFERENCES

Allison, J.D. & Allison, T.L. (2005). *Partition Coefficients for Metals in Surface Water, Soil, and Waste.* EPA/600/R-05/074.

ARCADIS. (2023). *Operable Unit 6 Remedial Investigation Data Evaluation Meeting #2. Vineland Chemical Company Superfund Site* [PowerPoint slides]. Presentation presented on December 8, 2023.

Chapra, S.C. (1997). *Surface Water-Quality Modeling*, McGraw-Hill Companies, Inc.

Donigian Jr., A. S., Bicknell, B. R., & Imhoff, J. C. (1995). Hydrologic Simulation Program - FORTRAN. *Computer Models of Watershed Hydrology*, Water Resources Publications, V. P. Sirgh, ed., Highlands Ranch, CO, 395-442.

Duda, P.B., Hummel, P.R., Donigian Jr, A.S., Imhoff, J.C. (2012). BASINS/HSPF: Model Use, Calibration, and Validation. *Journal of the ASABE*. Retrieved from: https://elibrary.asabe.org/abstract.asp?aid=42261&t=2&redir=&redirType=

DSI, LLC. (2024). EEMS - EFDC+ Explorer Modeling System. DSI LLC. Retrieved from: https://dsi.llc/eems

DSI, LLC. (2020). EFDC+ Theory. DSI, LLC. Version 10.2. Retrieved from: https://www.eemodelingsystem.com/wp-content/uploads/EFDC_Theory_Document_Ver_10.2_2020.05.21.pdf

Dzombak, D.A. & Morel, F.M.M. (1990). *Surface Complexation Modeling: Hydrous Ferric Oxide.* New York: John Wiley & Sons. (pp. 393).

GeoTrans, Inc. (2011). Report of the Remediation System Evaluation. Vineland Chemical Company Superfund Site, Vineland, NJ. Retrieved from: https://www.epa.gov/sites/default/files/2015-07/documents/vineland-rse-final.pdf

Hamrick, J. M. (1992). A Three-Dimensional Environmental Fluid Dynamics Computer Code: Theoretical and Computational Aspects. The College of William and Mary, Virginia Institute of Marine Science, Special Report 317. (pp. 63).

Hamrick, J.M. (2007). The Environmental Fluid Dynamics Code Theory and Computation. Volume 1: Hydrodynamics and Mass Transport. Tetra Tech, Inc., Fairfax, VA.

Harbaugh, A.W. (2005). MODFLOW-2005: The U.S. Geological Survey Modular Ground-Water Model -- The Ground-Water Flow Process: U.S. Geological Survey Techniques and Methods 6-A16. Retrieved from: https://pubs.usgs.gov/publication/tm6A16

Hayter, E.J., et al. (2006). Evaluation of the State-of-the-Art Contaminated Sediment Transport and Fate Modeling System. EPA/600/R-06/108. Ecosystems Research Division, National Exposure Research Laboratory, U.S. Environmental Protection Agency.

Hayter, E.J., et al. (2014). PCB Transport and Fate Modeling at New Bedford Harbor, MA. ERDC Letter Report. Vicksburg, MS: United States Army Corps of Engineers

HDR OBG. (2022). OU4 Surface Water and Sediment Phase 1 Remedial Investigation Data Evaluation Meeting [PowerPoint slides].

Karamalidis, A.K. & Dzombak, D.A. (2010). *Surface Complexation Modeling: Gibbsite.* Hoboken, NJ: John Wiley and Sons, Inc.

Keimowitz, A.R., et al. (2005). Arsenic Redistribution Between Sediments and Water Near a Highly Contaminated Source. *Environmental Science & Technology* (Vol. 39, No. 22, pp. 8606-8613).

Lockheed Martin SERAS. (2015). Technical Memorandum Maurice River Arsenic Investigation, Vineland, New Jersey, Work Assignment SERAS-185. Edison, NJ.

Mamindy-Pajany, J. (2009). Arsenic Adsorption onto Hematite and Goethite. *Comptes Renus Chimie* (Vol. 12, Issue 8, pp. 876-881). Retrieved from: https://www.sciencedirect.com/science/article/pii/S1631074808002312

McNeil, J., Taylor, C., & Lick, W. (1996). Measurements of Erosion of Undisturbed Bottom Sediments with Depth. *ASCE Journal of Hydraulic Engineering* (Vol. 122, Issue 6, pp. 316-324).

Murdoch, L. (2023). Clemson University Hydrograph Analysis [Microsoft Excel spreadsheet].

New Jersey Department of Environmental Protection (NJDEP). (2019). Export Image (Elevation/SJ_DEM). Retrieved from: https://maps.nj.gov/arcgis/rest/services/Elevation/SJ_DEM/ImageServer/exportImage?bbox=189722.0,34292.0,623544.0,488014.0

Ortiz-Letechipia, J., et al. (2022). Arsenic Speciation with Hydrogeochemical Modeling and Correlation with Fluorine in Groundwater in a Semiarid Region of Mexico. *Water* (Vol. 14, Issue 4, pp. 519). Retrieved from: https://doi.org/10.3390/w14040519

Parkhurst, D.L. & Appelo, C.A.J. (2013). Description of Input and Examples for PHREEQC Version 3—A Computer Program for Speciation, Batch-Reaction, One-Dimensional Transport, and Inverse Geochemical Calculations: U.S. Geological Survey Techniques and Methods, book 6, chap. A43, pp. 497. Retrieved from: https://doi.org/10.3133/tm6A43

Powell, B.A., Kersting, A., Zavarin, M., & Zhao, Plhong. (2008). Development of a Composite Non-Electrostatic Surface Complexation Model Describing Plutonium Sorption to Aluminosilicates. Lawrence Livermore National Laboratory.

RESPEC. (2024). Hydrologic Simulation Program-FORTRAN (HSPF). Retrieved from: https://www.respec.com/product/modeling-optimization/hydrologic-simulation-program%E2%80%91fortran/

Sea Engineering Inc. (2013). Union Lake Sedflume Analysis, Millville, NJ.

Sehayek, L., et al. (2014). Optimization of Remedial Action of Arsenic in Groundwater Vineland Chemical Co. Superfund Site, New Jersey, Part II: Column Tests Results, Platform Presentation, 2014-Contaminated Site Management: Sustainable Remediation & Management of Soil, Sediment and Water, November 17-20, 2014, San Diego, CA.

Shirinian-Orlando, A.A. & Uchrin, C.G. (2006). Modeling the Hydrology and Water Quality Using BASINS/HSPF for the upper Maurice River Watershed, New Jersey. Department of Environmental Sciences, Rutgers University, New Brunswick, NJ. Journal of Environmental Science and Health - Part A Toxic/Hazardous Substances and Environmental Engineering, (Vol.42, Issue 3, pp. 289-303). Retrieved from: https://doi.org/10.1080/10934520601134254

Smith, S.J., & Friedrichs, C.T. (2015). Image Processing Methods for In-Situ Estimation of Cohesive Sediment Floc Size, Settling Velocity, and Density. Association for the Sciences of Limnology and Oceanography. *Limnology and Oceanography: Methods* (Vol. 13, Issue 5, pp. 250-264).

United States Army Corps of Engineers (USACE) Philadelphia District. (2023). DRAFT 2022 Sampling Summary Annual Report Vineland Chemical Company Superfund Site, Vineland, New Jersey.

United States Environmental Protection Agency (USEPA). (2000). BASINS Technical Note 6. Estimating Hydrology and Hydraulic Parameters for HSPF. Retrieved from: https://www.epa.gov/sites/default/files/2015-08/documents/2000_08_14_basins_tecnote6.pdf

United States Environmental Protection Agency (USEPA). (2019). BASINS 4.5 (Better Assessment Science Integrating point & Non-point Sources) Modeling Framework. National Exposure Research Laboratory, RTP, North Carolina.

United States Environmental Protection Agency (USEPA). (2011). 5 Year Review Report. Vineland Chemical Company Superfund Site. Retrieved from: https://semspub.epa.gov/work/02/112016.pdf

United States Environmental Protection Agency (USEPA). (2023). Hydrological Simulation Program-FORTRAN (HSPF). Hydrologic Modeling Community of Practice. Retrieved from: https://www.epa.gov/ceam/hydrological-simulation-program-fortran-hspf

United States Environmental Protection Agency (USEPA). (2024). Superfund Site: Vineland Chemical Co., INC. Vineland, NJ. Retrieved from: https://cumulis.epa.gov/supercpad/SiteProfiles/index.cfm?fuseaction=second.cleanup&id=0200209

United States Environmental Protection Agency (USEPA). (2024b). Superfund Site: Former Kil-Tone Company Vineland, NJ. Retrieved from: https://cumulis.epa.gov/supercpad/SiteProfiles/index.cfm?fuseaction=second.Cleanup&id=0200874#bkground

United States Geological Survey (USGS). (2024). Maurice River at Norma NJ – 01411500. USGS Water Data. Retrieved from: https://waterdata.usgs.gov/monitoringlocation/01411500/#parameterCode=00060&showMedian=false&startDT=2012-01-01&endDT=2012-07-31

United States Geological Survey (USGS). (1976). Organic Carbon and Nitrogen Concentrations and Annual Organic Carbon Load of Six Selected Rivers of the United States. Geological Survey Water – Supply Paper 1817-F. Retrieved from: https://pubs.usgs.gov/wsp/1817f/report.pdf

Van Rijn, L.C. (1984). Sediment Transport: part I: bedload transport; part ii: suspended load transport: part iii: bed forms and alluvial roughness. *Journal of Hydraulic Engineering* Vol. 110, Issue 10, pp. 1431-1456; Vol. 110, Issue 11, pp. 1613-1641; Vol. 110, Issue 12, pp. 1733-1754.

Wesselink, A.J. and Gustard, A. (1992). Groundwater Storage in Chalk Aquifers – Estimation from Hydrographs. Institute of Hydrology. Retrieved from: https://nora.nerc.ac.uk/id/eprint/15334/1/N015334CR.pdf

Weston Solutions, Inc (WESTON). (2004). Model Calibration: Modeling Study of PCB Contamination in the Housatonic River. Prepared for U.S. Army Corps of Engineers and U.S. Environmental Protection Agency. DCN GE-122304-ACMG.

World Health Organization (WHO). (2024). Arsenic Fact Sheet. Retrieved from: https://www.who.int/news-room/fact-sheets/detail/arsenic#:~:text=Long%2Dterm%20exposure%20to%20arsenic,increased%20deaths%20in%20young%20adults.